

EUR 25.e

EUROPEAN ATOMIC ENERGY COMMUNITY – EURATOM

HEAVY WATER LATTICE BUCKLING MEASUREMENTS

by

R. BONALUMI and G.B. ZORZOLI

1962



RESEARCH AND DEVELOPMENT PROGRAM
EURATOM-CANADA

Special Technical Progress Report No R 46
established by CISE - Centro Informazioni Studi Esperienze
under the Euratom Contract No 012-60.12 Orgi

LEGAL NOTICE

This document was prepared under the sponsorship of the Commission of the European Atomic Energy Community (Euratom).

Neither the Euratom Commission, its contractors nor any person acting on their behalf:

- 1° — Make any warranty or representation, express or implied, with respect to the accuracy, completeness, or usefulness of the information contained in this document, or that the use of any information, apparatus, method, or process disclosed in this document may not infringe privately owned rights; or
- 2° — Assume any liability with respect to the use of, or for damages resulting from the use of any information, apparatus, method or process disclosed in this document.

This report can be obtained, at the price of Belgian Francs 50, from: PRESSES ACADEMIQUES EUROPEENNES, 98, chaussée de Charleroi, Brussels (Belgium).

Please remit payments:

- to BANQUE DE LA SOCIETE GENERALE (Agence Ma Campagne) account No. 964.558,
- to BELGIAN AMERICAN BANK and TRUST COMPANY - New York - account No 121.86,
- to LLOYDS BANK (Foreign) Ltd. - 10 Moorgate - London E.C. 2,

giving the reference: "EUR 25.e - Heavy Water Lattice Buckling Measurements".

Printed by Snoeck-Ducaju & Zoon. Brussels-Ghent. August 1962.

EUR 25.e

HEAVY WATER LATTICE BUCKLING MEASUREMENTS
by R. BONALUMI and G.B. ZORZOLI.

European Atomic Energy Community - EURATOM.
Centro Informazioni Studi Esperienze - CISE.
Final Report on contract No. 012-60.12 ORGI.

Brussels, August 1962 - pages 31 - Fig. 14.

A set of buckling measurements on Aquilon II, by replacement method is described. The tested configurations were made up of concentric annuli elements, fuelled by natural uranium metal and having polystyrene as simulating a homogeneous coolant.

The measured bucklings are compared with the calculated ones: the agreement is fairly good.

EUR 25.e

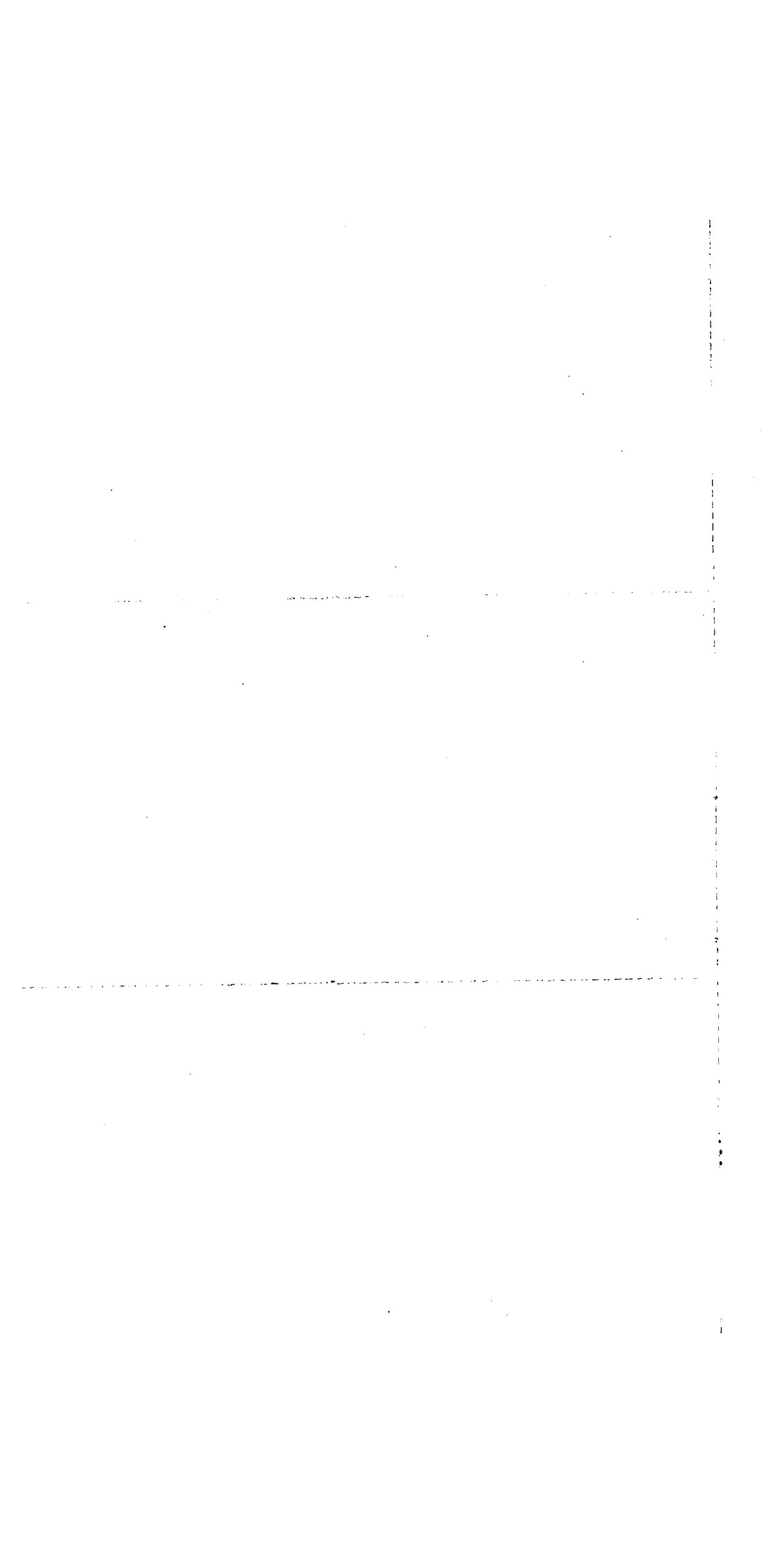
HEAVY WATER LATTICE BUCKLING MEASUREMENTS
by R. BONALUMI and G.B. ZORZOLI.

European Atomic Energy Community - EURATOM.
Centro Informazioni Studi Esperienze - CISE.
Final Report on contract No. 012-60.12 ORGI.

Brussels, August 1962 - pages 31 - Fig. 14.

A set of buckling measurements on Aquilon II, by replacement method is described. The tested configurations were made up of concentric annuli elements, fuelled by natural uranium metal and having polystyrene as simulating a homogeneous coolant.

The measured bucklings are compared with the calculated ones: the agreement is fairly good.



EUR 25.e

EUROPEAN ATOMIC ENERGY COMMUNITY – EURATOM

HEAVY WATER LATTICE BUCKLING MEASUREMENTS

by

R. BONALUMI and G.B. ZORZOLI

1962



RESEARCH AND DEVELOPMENT PROGRAM
EURATOM-CANADA

Special Technical Progress Report No R 46
established by CISE - Centro Informazioni Studi Esperienze
under the Euratom Contract No 012-60.12 Orgi

KEY TO THE TABLES

Table I	— Aquilon II reactor features	21
Table II	— 7 (OF ⁷) 7 element characteristics	21
Table III	— Effect of counters on reactivity	22
Table IV	— Reference lattice experimental data	22
Table V	— Results of substitution measurements	23
Table VI	— Numerical data of reference lattices	24
Table VII	— Computed data for ΔB^2 calculation	25
Table VIII	— Final results	25
Table IX	— Input data for buckling theoretical evaluation	26
Table X	— Theoretical cell parameters and bucklings of tested configurations	30
Table XI	— Comparison between calculated and experimental bucklings	30
Table XII	— Theoretical bucklings of the configurations used for studying the hydrogen effect	31

KEY TO THE FIGURES

Fig. 1	— Charging of fuel elements in Aquilon II	33
Fig. 2	— Fuel element hanging	34
Fig. 3	— Heavy water level variation system	35
Fig. 4	— Neutron detection system	36
Fig. 5	— Reference lattice fuel element	37
Fig. 6	— AC-1 element cross section	38
Fig. 7	— AC-2 element cross section	38
Fig. 8	— AC-1 top view	39
Fig. 9	— AC-2 top view	40
Fig. 10	— Critical height vs. number of replaced elements	41
Fig. 11	— Reflector coefficients vs. δH , 10 cm lattice pitch	41
Fig. 12	— Reflector coefficients vs. δH , 21 cm lattice pitch	42
Fig. 13	— Reflector coefficients vs. δH , 24 cm lattice pitch	42
Fig. 14	— AC-2-T-1 and AC-1-T-3 experimental bucklings vs. V_m/V_u	43

HEAVY WATER LATTICE BUCKLING MEASUREMENTS

SUMMARY

A set of buckling measurements on Aquilon II, by replacement method is described. The tested configurations were made up of concentric annuli elements, fuelled by natural uranium metal and having polystyrene as simulating a homogeneous coolant.

The measured bucklings are compared with the calculated ones: the agreement is fairly good.

INTRODUCTION

The work described in this report is in connection with contract n° 012-60.12 ORGI, between EURATOM and CISE, which lies within the framework of Euratom-Canada Research and Development Program.

Scope of the present contract is to study natural uranium fuelled, heavy water moderated lattices with different hydrogen contents in the coolant channels.

The present report is firstly devoted to describing the experimental procedures and the desired results derived therefrom; a general discussion on such results follows, along with a comparison with calculated bucklings for the same configurations.

1 — MEASUREMENT PRINCIPLES

Heavy water lattice bucklings are measured on Aquilon II by the substitution method (1). The principle in this method consists in measuring the difference in buckling between the configuration under test and a reference lattice whose buckling is already known.

Then the experimental technique consists of two subsequent steps:

a) determination of the reference lattice buckling by flux mapping a critical assembly fully made up of that lattice;

b) determination of buckling difference ΔB^2 between reference and tested lattices by means of proper experimental techniques, associated with a theoretical interpretation of these measurements.

Point b) will be outlined in some details as follows. One first takes into consideration the reference lattice, then the lattice with the four central elements being replaced by elements of the configuration to be tested, and subsequently the configurations where the 12, the 16, the 24 central elements of the reference lattice are replaced.

For each of the aforesaid configurations, critical height is determined as follows: for some heavy water levels (generally four), for which the system is supercritical, the stable doubling time is measured. Since heights are so chosen as to obtain doubling times in the range between about 10 and 100 seconds, the relationship between heavy water level and reactivity (derived from the doubling time by means of Nordheim's formula) is actually linear, so that critical height can be evaluated by extrapolation to zero reactivity.

Critical height is the only parameter involved in the interpretation of experiments, along with reference lattice radial and axial bucklings (β_o^2 and α_o^2 respectively) measured as pointed out in a). The practical formulae used to calculate ΔB^2 are listed below:

$$R_o = d \sqrt{\frac{n}{\pi}} \quad (1)$$

$$R_1 = d \sqrt{\frac{N}{\pi}} \quad (2)$$

$$\beta^2 = \beta_o^2 + \frac{1 + e''}{1 + e'} \left[\frac{\pi^2}{H_e^2} - \frac{\pi^2}{(H_e + \delta H)^2} \right] \quad (3)$$

$$\beta'^2 = \beta^2 + \frac{\Delta B^2}{1 + e'} \quad (4)$$

$$\beta_o^{*2} = \beta_o^2 - e (\beta^2 - \beta_o^2) \quad (5)$$

$$\gamma^2 = \frac{1}{L_i^2} + \frac{1}{L_r^2} + 2 \left(\beta_o^2 + \frac{\pi^2}{H_e^2} \right) - \beta^2 \quad (6)$$

$$\gamma'^2 = \frac{1}{L_i'^2} + \frac{1}{L_r'^2} + 2 \left(\beta_o^2 + \frac{\pi^2}{H_e^2} - \Delta \beta^2 \right) - \beta'^2 \quad (7)$$

$$\Lambda = \frac{1}{\beta'} \left(\frac{J_o}{J_1} \right)_{\beta R_o} \quad (8)$$

$$\Lambda' = \frac{1}{\gamma'} \left(\frac{I_o}{I_1} \right)_{\gamma R_o} \quad (9)$$

$$\Lambda_1^* = \frac{1}{\beta_o^*} \left(\frac{J_o}{J_1} \right)_{\beta_o^* R_1} \quad (10)$$

$$U = \left(\frac{Y_o - \beta \Lambda Y_1}{J_o - \beta \Lambda J_1} \right)_{\beta R_o} \cdot \left(\frac{J_o - \beta \Lambda_1^* J_1}{Y_o - \beta \Lambda_1^* Y_1} \right)_{\beta R_1} \quad (11)$$

$$V = \left(\frac{J_o - \beta \Lambda' J_1}{J_o - \beta \Lambda J_1} \right)_{\beta R_o} \cdot \left(\frac{K_o - \gamma \Lambda K_1}{K_o - \gamma \Lambda' K_1} \right)_{\gamma R_o} \quad (12)$$

For each substitution U and V must be calculated with the above procedure. R_o and R_1 are radii of the equivalent cylinders corresponding to the replacement section of the core (containing n substituted elements) and the whole core (containing N cells); d is the lattice pitch. The "reflector coefficients" e , e' e'' are defined as:

$$e = \frac{\partial \beta^2}{\partial \alpha^2} \quad \text{with a constant core radius}$$

$$e' = \frac{\partial \alpha^2}{\partial \beta^2} \quad \text{with a constant critical height}$$

$$1+e'' = \frac{\partial H_e}{\partial H} \quad \text{with a constant radial buckling}$$

where:

$$\beta^2 = \text{radial buckling}$$

$$\alpha^2 = \text{axial buckling}$$

$$H_e = \text{core extrapolated height}$$

$$H = \text{core critical height.}$$

The actual calculation of e , e' and e'' will be illustrated in sec. 5. R_o and R_1 are readily evaluated by Eqs. (1) and (2).

In Eq. (3), besides the already defined quantities, H_e is the reference lattice extrapolated height ($= \frac{\pi}{\alpha_o}$), whereas δH is the difference between the critical height of the particular substitution and the one of the reference lattice, derived as described at point b).

Once β^2 is known, Eqs. (4) and (5) provide β'^2 and β_o^{*2} , when a trial value for ΔB^2 is introduced into Eq. (4). Furthermore, the calculation of γ and γ' requires the values of L_i^2 , L_r^2 , $L'_i{}^2$, $L'_r{}^2$ which are diffusion and slowing-down areas for the reference and tested lattice respectively: these values are calculated beforehand.

Finally, the use of Eqs. (8) through (10) gives input data for calculating U and V .

When the four couples of (U,V) values are available for the whole set of substitution, they are inserted into the following equation

$$\rho = U + VS \quad (13)$$

In this equation, S is a known function of the coupling coefficients of both reference and tested lattices, but its numerical evaluation is highly uncertain, so that, in Eq. (13), both ρ and S are adjusted as unknown quantities by a least square method.

ρ is an iteration factor which, when multiplied by the trial ΔB^2 value, gives the first iteration ΔB^2 . This procedure is repeated until the difference between two successive values of ΔB^2 is less than a desired quantity.

Once ΔB^2 is known, the tested lattice buckling is readily available as

$$B^2 = \beta_o^2 + \alpha_o^2 + \Delta B^2 \quad (14)$$

2 — EXPERIMENTAL FACILITY

In this section some operating characteristics of Aquilon II will be mentioned in order to facilitate a general understanding of this work.

Aquilon II is essentially made up of a cylindrical aluminum tank, which contains the reactor core, i.e. heavy water and fuel elements; the tank is surrounded by side and bottom graphite reflectors.

Dimensions and other features are reported in Table I.

Fuel elements are suspended by means of metallic ropes screwed into proper fuel element top threads, through a metallic holder (Fig. 1). A rider at the rope top leans upon one of the cross bars hanging over D_2O , as shown in Fig. 2.

Movement of cross bars on rolling bearings, and displacement of riders along cross bars allow a quick change of lattice pitch.

Heavy water level in the tank is the only variable with which one deals to change the neutron balance of the system. The level may be varied by simply pumping heavy water in or out.

However, when well-defined steps in water level are needed, as for instance in determining critical height by successive divergences (see Sec. 1), the following system is used (see Fig. 3): heavy water is pumped from the reactor tank to a level control tank with a capacity limited to a maximum of 40 l because of the presence of a spillway. On the other hand, water can be evacuated from the level control tank through any of valves *A*, *B*, *C* and *D*, and sent either back to the reactor tank or to the hold-up tank, depending upon the position of the two-way valve *E*. The quantity of water contained between spillway and each evacuation valve level is known to be:

5 l	down to	<i>A</i>	valve level;
10 l	»	»	<i>B</i> » » ;
20 l	»	»	<i>C</i> » » ;
40 l	»	»	<i>D</i> » » .

Therefore, to get a known variation of heavy water content in the reactor tank, e.g. 20 l, one fills up the level control tank, then evacuates through *C* back to the reactor tank, and finally, through *D*, to the hold-up tank.

As for the heavy water level measurement, two different gages are available: the first, the use of which was started just after the beginning of the experiments herein reported, is an electric device giving an accuracy in level within ± 0.1 mm; the second is an optical device of a rather inaccurate reading (up to errors of 2-3 mm).

Daily temperature measurements inside the tank were made by means of six thermocouples, with an accuracy within 0.1 °C.

Periodical checks of heavy water isotopic composition were also performed.

Since the height of the multiplying medium is effectively limited by heavy water level, the same effective height is achieved in the side graphite reflector by inserting, from the top, a cadmium cylindrical sheet between tank and graphite, with the lower edge being at the heavy water level.

As for control system, see Table I.

Neutron detection is ensured by four B_4C ionization chambers, symmetrically placed into the side graphite reflector, and by one B_4C chamber and two BF_3 counters, centrally placed into the bottom reflector, just below the reactor tank.

Fig. 4 shows a block diagram of the detection chains. Particularly important for experiments is the bottom B_4C chamber, which is connected to the doubling time measurement device.

The latter consists of 10 doubling time meters, the first of which is automatically triggered when a prefixed flux level is reached (so as to be roughly in stable period conditions), whereas the remaining chains are sequentially triggered with such delays that the full measurement covers 5.5 doubling times.

3 — REFERENCE LATTICE MEASUREMENTS

The reference lattice (*) was made up of fuel elements of the type shown in Fig. 5, hereinafter named “7(O F)7”, according to the denomination used by Aquilon’s staff.

This fuel element is a seven UO_2 rods cluster with the characteristics listed in Table II.

112 “7(O F)7” elements were used as a reference lattice in Aquilon II, regardless of lattice pitch. Therefore, because of the Aquilon dimensions (see Table I), for the three chosen lattice pitches the following situations occurred:

- lattice pitch 19 cm: a heavy water radial reflector about 31 cm thick between core and graphite radial reflector;
- lattice pitch 21 cm: a heavy water radial reflector about 19 cm thick between core and graphite radial reflector;
- lattice pitch 24 cm: heavy water tank filled up with core lattice, hence no heavy water reflector at this pitch.

As explained in Sec. 1, reference lattice bucklings were measured by flux mapping, which is achieved by means of Mn detectors, 6.15 mm in diameter, 0.5 mm thick. Such detectors are horizontally placed inside watertight aluminum tubes, 7.5 mm *ID*, 9 mm *OD*, 2 m long; Mn positioning inside the tubes is ensured by aluminum spacers, 5-10 or 15 cm long, provided with suitable housing to hold detectors.

Bi slugs in the bottom serve as ballasts to ensure verticality of tubes, which are hung along the straight line common to four adjacent elementary cells.

Detector irradiation is performed as follows:

a) Heavy water level is fixed higher than critical so as to give a doubling time longer than 100 s, with the Cd control plates withdrawn;

b) Once the Cd control plates are withdrawn, divergence is allowed for about 15 minutes, until a 25-30 W power is reached; then the reactor is shut down.

In this way, the flux shape, during irradiation, is not perturbed by the presence of control elements.

(*) Throughout this report, all lattices should be understood to be square.

Detector β^- decay is counted in 8 counting chains, which may consist of either *G.M.* tubes or crystals, connected with proper electronics.

8 detectors are counted at a time, and so rotated that each detector is counted by all of 8 chains.

The raw results must be elaborated to take into account several factors, such as the delay between different sets of 8 detectors, the counting sequence of each detector in the 8 counting chains, detector and counter efficiencies, background, dead time, and so on.

All the data necessary for such elaboration are automatically punched so as to feed directly an IBM 7090 digital computer, which gives as outputs the net counting rate (*cpm*) for each detector.

The number of detectors in each irradiation batch was 40 or 48. The first case corresponds to the use of 4 aluminum tubes each containing 10 detectors (thus experimental data for evaluating axial buckling only were available); the second case corresponds to the use of either 8 aluminum tubes with 6 detectors each, or 6 aluminum tubes with 8 detectors each (thus experimental data for evaluating both axial and radial buckling were available).

7 irradiations were performed for each reference lattice pitch, and for three different pitches (19, 21 and 24 cm.).

The net counting rates are used as input data for an IBM 7090 least square program, which fits the aforesaid data to the general formula of neutron flux in a cylindrical reactor:

$$0 = AJ_o(\beta r) \sin(\alpha z - \gamma) \quad (15)$$

where $\beta = \frac{2.405}{R_e}$, $\alpha = \frac{\pi}{H_e}$, R_e and H_e being extrapolated radius and height respectively.

At any run the program may adjust one of the following groups of parameters in Eq. (15):

A and α ; A and β ; A , α and γ ; A , β and α ; A , β , α and γ .

The scope of the program is to minimize the following expression

$$\sum_i p_i \{ O_i - \rho AJ_o [(\beta + \delta\beta) r_i] \sin [(\alpha + \delta\alpha) z_i - (\gamma + \delta\gamma)] \}^2 \quad (16)$$

where O_i is the counting rate at the point (r_i, z_i) .

The terms of expression (16) are expanded to the 1st order of a Taylor series, whose derivatives with respect to ρ , $\delta\alpha$, $\delta\beta$, $\delta\gamma$ are set equal to zero; the consequent system of equations can then be solved for ρ , $\delta\alpha$, $\delta\beta$, $\delta\gamma$ with given values of A , α , β , γ . The linearization of the problem requires an iterative procedure: iterations go on with $p_i = 1$ as long as one at least of the values $1 - \rho$, $\delta\alpha$, $\delta\beta$, $\delta\gamma$ is greater than 10^{-3} ; when this precision is achieved, a further iteration is performed assuming $p_i = \frac{1}{\sigma_i^2}$, σ_i being the deviation between counting rate at the point (r_i, z_i) and the corresponding fit value.

The heavy water level, at which irradiations are performed, is higher than the critical one for a clean lattice. In fact, irradiation is made in divergent conditions, i.e. with a supercritical height, and several extra-absorbers are present: detectors and aluminum tubes, and all chambers and counters (see Sec. 2).

For these reasons, every calculated α gives a value

$$H_c^* = \frac{\pi}{\alpha}$$

which must be corrected.

A first correction consists in deducing, from H_e^* , the difference between the irradiation heavy water level and the critical one, the latter being determined according to the procedure described in Sec. 1, point b).

The reactivity absorbed by chambers, counters and aluminum tubes, is determined by measuring the change in doubling time when the particular perturbing element is withdrawn from the system.

As pointed out before, Nordheim's formula gives reactivity as a function of doubling time; on the other hand, divergence measurements that give the critical height, also furnish the number of pcm per mm of heavy water level, as the slope of the straight line correlating reactivity and height. Consequently, the reactivity absorbed by parasitic elements is easily converted into the equivalent heavy water height to be also subtracted from H_e^* .

Table III summarizes the effects of counters on reactivity for the three tested reference lattices.

A further step is to average the different extrapolated radii (R_e) and heights (H_e) coming from single best fits. Since the number of irradiations and therefore of R_e and H_e values are limited, an evaluation of the confidence limit of the average values is possible by the use of Student's law; in particular, uncertainties corresponding to confidence limits of 95 and 99 % were calculated here.

A different approach, consisting in developing a least square calculation in which the uncertainty of every experimental point is accounted, does not look feasible here; in fact, standard deviation is always very small, whereas major sources of error are: position of cross bars and riders (and therefore radial position of detectors as well as fuel rods) which may be wrong by 1 mm at least; the non-perfect stiffness of suspensions, which may alter detector axial position by $2 \div 3$ mm, as well as the distance from fuel element to tank bottom; changes in D_2O temperature in different irradiations, and so on.

All of these different sources of error cannot be accounted for in a systematic way.

Moreover, a preliminary screening was achieved by repeating computer runs discarding particular experimental points too widely deviated from fitting curves.

Once α^2 and β^2 are known, the consequent buckling values, which correspond to particular heavy water isotopic purities, are so corrected as to refer all values to a 99.8 % D_2O fraction.

Such results are still to be corrected for temperature deviations from the 20 °C reference temperature assumed in theoretical calculations. These deviations were accounted for by simply averaging single run temperatures (assumed with a unit statistical weight) to a value \bar{T}_m , whence a variation in buckling can be derived as:

$$\delta B^2 = -\frac{2\pi^2}{H_e^3} \frac{dH_e}{d\rho} \frac{d\rho}{dT} (\bar{T}_m - 20^\circ\text{C})$$

(where ρ is reactivity) if one assumes that it can be compensated just by changing heavy water level: $\frac{d\rho}{dT}$ is 20 pcm/°C, whereas $\frac{d\rho}{dH}$ is given in Table III.

Final results are reported in Table IV.

4 — REPLACEMENT MEASUREMENTS

Replacement measurements were performed on 9 different configurations. Two types of fuel element were used: one, named AC-1, is shown in Fig. 6, while the other, named AC-2, is shown in Fig. 7.

Figs. 8 and 9 are pictures presenting AC-1 and AC-2 element top views respectively: white rods and tubes are of polystyrene simulating the homogeneous coolant. Polystyrene, when present, may have two different densities: 0.307 g/cm^3 and 0.578 g/cm^3 (average values). Listed below are the nine tested configurations according to the assumed nomenclature:

- AC-1-T-0-21: AC-1 element, no polystyrene, 21 cm lattice pitch
- AC-1-T-1-21: AC-1 element, low density polystyrene, 21 cm lattice pitch
- AC-1-T-3-19: AC-1 element, high density polystyrene, 19 cm lattice pitch
- AC-1-T-3-21: AC-1 element, high density polystyrene, 21 cm lattice pitch
- AC-1-T-3-24: AC-1 element, high density polystyrene, 24 cm lattice pitch
- AC-1-S-3-21: AC-1 element with inner Al tube removed, high density polystyrene, 21 cm lattice pitch
- AC-2-T-1-19: AC-2 element, low density polystyrene, 19 cm lattice pitch
- AC-2-T-1-21: AC-2 element, low density polystyrene, 21 cm lattice pitch
- AC-2-T-1-24: AC-2 element, low density polystyrene, 24 cm lattice pitch

Besides measurement principles described in Sec. 1, it is worthwhile to emphasize some details concerning experiments.

As far as the doubling time determination is concerned, to be sure that the stable divergence is achieved, results given by the four or five last chains only are averaged to give the accepted doubling time. Useful results are selected backward beginning from the last value, the values being limited to data not deviating too far from the average value of the subsequent chains.

At any rate, one must recall that the uncertainty in the doubling time meter data is within 1 %.

Heavy water level, as pointed out before, can be determined by optical or electric means: the former was used in AC-1-S-3-21 measurements only, the latter throughout the rest of experiments.

Since most replacements lasted longer than one day, an intercalibration was necessary. In fact, core temperature could appreciably change from one day to another, and moreover the optical reading of the water level, besides its parallax error, was affected by the fact that the water in the level gage followed more rapidly the change in room temperature than it did in the reactor tank.

Therefore, so long as level was read optically, and until sufficient confidence in electrical reading was finally achieved, intercalibration was obtained by repeating at any one day the last substitution of the day before, and using the two critical heights so obtained for intercalibrating the whole set.

Later on, calibration was made simply by taking into account changes in core temperature from one day to another: in fact, that was the only variable, because the electrical reading could be well reproduced. Due to the small changes in temperature, the rough value of $20 \text{ pcm}/^\circ \text{C}$ was abundantly sufficient to give the change in reactivity ρ ,

which was converted into the corresponding change in height H , with the use of the $\frac{\partial \rho}{\partial H}$ value derived from divergence measurements belonging to that day.

The ρ_i and H_i values derived from a single substitution were fit by a least-square method, according to the formula:

$$\rho = a H + b \quad (17)$$

which gives

$$a = \frac{d\rho}{dH} = \frac{n \sum_{i=1}^n H_i \rho_i - (\sum_{i=1}^n \rho_i)(\sum_{i=1}^n H_i)}{n \sum_{i=1}^n H_i^2 - (\sum_{i=1}^n H_i)^2} \quad (18)$$

$$H_c = -\frac{b}{a} = \frac{1}{n} \left\{ \sum_{i=1}^n H_i - \frac{\sum_{i=1}^n \rho_i}{a} \right\} \quad (19)$$

where n is the number of divergences and H_c is the critical height.

The mean square deviation of H_c is determined by calculating

$$\frac{1}{n} \sum_{i=1}^n \left(H_i - \frac{\rho_i - b}{a} \right)^2 = \sigma_H^2$$

Table V summarizes, for each configuration, critical heights, their mean deviations (rounded off to the first decimal figure) and the difference from the reference critical height, for all substitutions.

As can be seen, nearly all substitutions are very close to the reference lattice; thus one can have a priori a reasonable confidence in the results.

A further check consists in plotting H_c against the number of replaced elements: as shown in fig. 10 for two particular cases, the relationship is linear, as expected from the relatively small perturbations of the reference lattice.

5 — INTERPRETATION OF EXPERIMENTAL DATA

Interpretation of experimental data, as already elaborated in secs. 3 and 4, was further carried on by means of the recipe described in detail in sec. 1 (formulae (1) through (13)).

Actually such calculations were carried out making use of a proper IBM 7090 code, available at Saclay. As far as input data are concerned, they can be divided into four groups.

The first of these groups includes trivial input data, such as for instance total number of fuel elements in the lattice, number of replaced fuel elements, lattice pitch.

The second is limited to the three data derived from experimental results, and entering formulae (3) through (7), i.e. reference lattice radial buckling, reference lattice

extrapolated length, difference between substituted and reference lattice critical height.

The third group includes numerical data related to the reference lattices; thermal diffusion area and slowing down area were calculated by desk computer, according to standard calculation recipes used at Saclay. On the other hand, the accuracy needed is rather low, since an error up to 10 % can be accepted without altering sensitively the final results.

All the other data concerning the three reference lattices were calculated following the same recipes and are here reported in table VI. Such data are used as inputs into a two group multi-region program (2), which allows the evaluation of the reflector coefficients. This is practically done as follows: in the case of

$$e = \left(\frac{\partial \beta^2}{\partial \alpha^2} \right)_{R=const.}$$

for instance, criticality calculations are performed for different extrapolated heights of the reference lattice, at constant core radius so as to get the corresponding values of β^2 . Similar calculations are made in the case of e' and e'' .

In all of the three cases, for each reference lattice, the actual extrapolated height is used as zero, and so e , e' , e'' are known for some deviations (δH) from such height as incremental ratios. Figs. 11 through 13 are plots of the calculated values for the three reference lattices here utilized vs. δH .

Since the substitution configurations are all rather similar to their own references, one can reasonably assume that such coefficients are still valid in substitutions, thus avoiding further calculations. In other words, e , e' , e'' for a reference lattice at a given lattice pitch are also used for all substitutions having the same lattice pitch, in the following simple way: by using plots of fig. 11 through 13 one evaluates e , e' , e'' corresponding to the δH_e for the particular substitution, as given in table V. In some cases, δH_e values were outside the calculated range for a reflector coefficient: then a linear extrapolation was used, which is also deemed reasonable because of the limited deviation of such cases from the calculated range.

The last group of numerical data includes thermal diffusion area and slowing down area for the configurations under study, which were taken from the preliminary calculations. As for the trial value of ΔB^2 , it was simply assumed to be equal to the difference between the preliminary data, and the reference lattice experimental data, as given in Table IV of the present report.

The program iterates until the difference between ΔB^2 values of the two last iterations is lower than 1/1000. Output data for each configuration are: the couples of (U , V) values for the four substitutions, the fitting ρ and S values (see Eq. (13)) and the two last calculated ΔB^2 s.

Table VIII lists, for all but one configurations, ρ , S and the last ΔB^2 , along with the mean deviation of the U values from the best fit straight line, and the corresponding deviations of ΔB^2 .

The only configuration absent from this table is AC-2-T-1-19; in fact, as shown in Table V, no significant variation from the reference lattice critical height was observed, and therefore it was assumed that $\Delta B^2=0$.

As can be seen, deviations of ΔB^2 are very small. On the other hand one must remember that these calculations made use of reference lattice extrapolated dimensions which are affected by uncertainties dependent upon the chosen confidence limit (see

Sec. 3). Because of that, calculations were also performed for H_e -values different from the average ones arising from flux-mapping, so as to evaluate the corresponding variations in ΔB^2 . Then variations in ΔB^2 were calculated for $H_e + \delta H$, δH being the deviation corresponding to a confidence limit of 99 %: they happened to be ranging from 1.06 to 2.70 % of ΔB^2 . No direct effect of radial dimension variations was calculated, nevertheless it seems reasonable to assume an effect of about the same value. As far as reflector coefficients are concerned, in Aquilon II they are much smaller than in Aquilon I, so that—due to the small ΔB^2 —their errors can be neglected.

Table VIII summarizes the results of these measurements: reference bucklings and their uncertainties, ΔB^2 and their uncertainties, tested lattice bucklings and their uncertainties. All uncertainties refer to a 99 % confidence limit.

As can be seen, uncertainties on ΔB^2 are quite negligible with respect to B^2 's uncertainties.

Fig. 14 is a plot of AC-2-T-1 and AC-1-T-3 experimental bucklings against V_m/V_u .

6 — THEORETICAL ANALYSIS

Preliminary buckling values for the nine tested configurations were calculated. They are to be considered as preliminary, the main goal being that of giving sufficient information for the choice of the experimental configurations from all the possible ones, as well as furnishing the data (thermal diffusion area, slowing down area) to be used in the frame of the interpretation of experimental results.

A quick comparison between such values and the experimental ones of Sec. 5 of the present report, shows that the former, even if preliminary, are already in fair agreement with the latter (see Table XI).

In what follows, some improvements in calculations will be described, and the consequent results reported.

It is worthwhile to emphasize that such improvements are simply related to a proper choice of numerical constants, since the theoretical model is the one coded for automatic computation, described in detail in Ref. 3.

A first change is in the calculation of the neutron temperature, which is evaluated as

$$T_n = T_m \left(1 + 0.92 \frac{A_m}{1-f} \frac{\sigma_{um}(k T_m)}{\sigma_{sm}} \right) \quad (20)$$

where:

- T_n = absolute neutron temperature;
- T_m = » moderator »
- A_m = mass number of moderator;
- f = thermal utilization factor of the lattice;

$\sigma_{am}(kT_m) =$ moderator microscopic absorption cross section point value at the energy kT_m ($k =$ Boltzmann constant)

$\sigma_{sm} =$ moderator microscopic scattering cross section just above thermal energies

In the preliminary study $(1-f)$ was assumed to be 0.05. The consequent calculations gave thermal utilization values for each region in the lattice, according to Amouyal and Benoist's theory. Therefore, these new values of f were introduced into Eq. (20) to get T_n .

A second change involves the homogeneous medium density. At the time input data for preliminary calculations were chosen, the actual average density for polystyrene pieces was known, whereas information on their tolerances, and therefore on air gaps between polystyrene and uranium within fuel elements, was still incomplete. Therefore, as a straight assumption, actual polystyrene density was used for the fuel element regions containing it. In practice, that resulted in a sensitive overestimate of polystyrene effect. In the present case polystyrene is diluted all over the corresponding regions, leading to values of 0.511 gr/cm² and 0.271 g/cm³ for higher and lower density respectively, against 0.578 and 0.307 g/cm³.

A third change is in the fast fission factor calculation, where neutron first collision probability is evaluated for neutrons generated with the same distribution of the thermal flux, further collision probabilities being for a flat neutron distribution. At the time preliminary calculations were performed, the automatic connection of the different sections in *Cocco Bill* had not yet been completed, so that information on thermal flux distribution, to-day automatically fed into the fast fission factor code by the thermal utilization factor code, was not available. Then provisional input data were chosen, assuming all generation neutrons uniformly distributed.

All other data and assumptions are unchanged. In particular, the 2200 m/s Aluminum capture cross section, which was previously taken as 0.23 b, was kept unaltered even after its experimental determination by oscillating methods on *Zoe* reactor at Fontenay-aux-Roses (4). In fact, several specimens gave scattered results around approximately 0.23 b, so that no change from the assumed value was justified on physical grounds.

Table IX lists the most significant input data for the nine configurations under study (the reported f -values are the ones assumed in calculating T_n) whereas table X gives all cell parameters of some interest. As one can see from table IX, no substantial change in input data comes from the small differences among the various neutron temperatures.

Table XI presents experimental and variously calculated bucklings. Two different calculations have been worked out:

a) making use of CISE correlation, described in Ref. 5, applied to physical data refined as explained above; the aforesaid correlation assumes the following values:

$$\left. \begin{array}{l} A = 2.3 \text{ b} \\ B = 11.285 \text{ b } \sqrt{\text{g/cm}^2} \\ y = 0.9686 \end{array} \right\} \begin{array}{l} \text{effective resonance} \\ \text{integral coefficients} \end{array}$$

to be introduced into the criticality equation:

$$y\eta_{calc}^{\epsilon f} = (1 + \beta^2 L_{rM}^2 + \alpha^2 L_{zM}^2) \left(\frac{1}{q} + \beta^2 L_{re}^2 + \alpha^2 L_{ze}^2 \right)$$

b) assuming $\gamma = 1$ and using Hellstrand's effective resonance integral correlation ($A = 2.81$; $B = 24.7$).

Just for the sake of comparison, the preliminary calculated values are also reported.

As can be seen from the table, the buckling values calculated after CISE correlation are in very good agreement with experiments: moreover, experimental and calculated values agree well within experimental uncertainties in all but three cases, the exceptions involving the AC-2 fuel element lattices. This is possibly due to neglecting the spectral hardening inside the central uranium rod; anyway, the deviation from experimental values, although apparently systematic, is not very serious, and allows good confidence in calculations in any case. In fact, the root of the mean square deviation between experimental and calculated bucklings over the nine tested configurations is 0.10 m^{-2} ; when calculated for the six AC-1 configurations only, the value drops down to 0.04 m^{-2} .

On the other hand, a very marked disagreement is evident between experiments and calculations b): the calculations always underestimate rather seriously the buckling, even though much of the discrepancy disappears at large lattice spacings, and when polystyrene is absent.

The latter case should be related to the noticeable difference between Hellstrand's and CISE correlation values of the coefficient B of the effective resonance integral: in the case where polystyrene is absent, the surface resonance absorption is of little importance, due to the small "effective surface", and differences in B also become less important than with polystyrene.

As a final conclusion, CISE correlation can be accepted with good reliability for criticality calculations on natural uranium fuelled, D_2O moderated lattices: however, the application of this correlation to other types of calculations (fuel cycles, etc.) is not justifiable on physical grounds.

Of some interest is the question of how accurately reactivity can be calculated for a power reactor, taking as a basis the experimental accuracy with which bucklings have been measured.

Consider for instance a power reactor with extrapolated radius $R_e = 300 \text{ cm}$ and extrapolated height $H_e = 450 \text{ cm}$: let the core consist of an AC-1-T-1-21 lattice, whose material buckling has been measured as $5.23 \pm 0.12 \text{ m}^{-2}$. The 0.12 m^{-2} uncertainty on the material buckling gives a corresponding uncertainty on reactivity for the cold clean reactor:

$$\delta\rho = 257 \text{ pcm}$$

This uncertainty is the highest among those calculated for the nine tested lattices, with the possible exception of the AC-1-T-0-21 core, whose uncertainty, evaluated as 261 pcm, is not fully reliable, because of the strong anisotropy featuring this lattice.

In any case, an uncertainty less than 300 pcm is quite acceptable for the design of a power reactor in which an initial reactivity of about 7000 pcm is desired.

7 — DIFFERENTIAL PARAMETERS FOR DESIGN CALCULATIONS

This section is aimed at discussing the possibility of deriving, from both experimental and theoretical results, some differential parameters for the sole purpose of providing approximate recipes for tentative evaluations.

For the time being, attention has been focused on two leading effects on buckling:

- a) "hydrogen effect",
- b) "structural material effect".

Concerning the first item, available experimental data are limited to the three measured bucklings for AC-1-T elements at 21 cm lattice pitch.

The only variable here is the hydrogen nuclear density N_H .

As a tentative approach, the experimental buckling variation with respect to the zero-hydrogen case, $B^2(0) - B^2(N_H)$, has been plotted vs. N_H , and it exhibited a linear trend. The slope of the straight line, i.e. $-\frac{\partial B^2}{\partial N_H}$, which is equal to $0.593 \text{ m}^{-2}/10^{22} \text{ cm}^{-3}$, has been compared with the one derived from the corresponding theoretical data (0.58), and no appreciable difference has been found, as the results shown in Sec. 6 would lead us to expect.

Because of this, it was considered sufficient for our purposes to base the analysis upon theoretical buckling values only: to do this, a number of lattices has been theoretically examined: the corresponding bucklings are shown in Table XII.

From these results one realizes what follows:

- a) fuel element and lattice pitch being fixed, the relationship between $B^2(0) - B^2(N_H)$ and N_H is linear;
- b) the values $\alpha_H = -\frac{\partial B^2}{\partial N_H}$ are ranging for the elements AC-1 from 0.58 (lattice pitch = 21 cm) to 0.45 (lattice pitch = 19) through 0.51 (lattice pitch = 24 cm);
- c) the values $\alpha_H = -\frac{\partial B^2}{\partial N_H}$ are all assembled for the elements AC-2 around 0.45.

A further step of this investigation consisted in looking for a general "hydrogen coefficient" which might apply to AC-1 as well as to AC-2 fueled lattices: many attempts have been made to correlate the buckling variation $B^2(0) - B^2(N_H)$ to some parameter involving, besides N_H , one or more of other quantities, such as the hydrogen volume, the fuel volume, the absorption cross sections of both hydrogen and fuel, and so on.

Unfortunately such efforts gave no result at all.

With regard to the variations in buckling induced by the presence of structural materials, experimental information is limited to the differential effect of an aluminum "pressure" tube between AC-1-T-3-21 and AC-1-S-3-21 configurations (this effect amounts to a buckling difference of 0.80 m^{-2}). However, as the preliminary calculations exhibited no wide variation in the buckling difference between AC-1-T and AC-1-S lattices when cell dimensions were varied (from a maximum of 0.87 m^{-2} at a 10 cm lattice pitch, down to

a minimum of 0.77 m^{-2} at 23 cm cell spacing), nor did they seriously depart from the only measured value, the latter has been assumed as a constant for a fixed pressure tube.

With this fact duly appreciated, it has been possible to assume as an independent parameter the sum of the products $\Sigma_{ao} V$ over all structural materials ($\Sigma_{ao} = 2200 \text{ m/s}$ macroscopic absorption cross section, $V = \text{volume}$): this makes it possible to deal with materials other than aluminum, provided their position in the fuel is the typical one of a pressure tube (it is not quite true that the same recipe also applies to materials otherwise placed), and provided their absorption cross section follows the $1/v$ law, at least approximately (in this case Σ_{ao} has the meaning of a Westcott cross section).

The following "structural material coefficient" has then been defined and evaluated after experiments:

$$\alpha_{str} = \frac{\partial B^2}{\partial (\Sigma_{ao} V)_{str}} = -10.89 \frac{\text{m}^{-2}}{\text{cm}}$$

Of course the aforesaid figures can be recognized as adequate enough only for the type of application for which they have been devised, i.e. rough preliminary evaluations; the main limitation, however, still lies in the fact that no generalization has yet been found for other fuel elements than those herein examined in detail.

Anyway the fair agreement between theoretical and experimental values will allow the direct evaluation of any effect for other configurations simply by theoretical calculations.

3 — CONCLUSION

The good agreement between theoretical data and experimental results, shown by the present report, gives a great deal of confidence in the recipe utilized for buckling calculation, at least within the configuration range taken into consideration.

Such agreement, however, must not conceal the substantial deviation from standard data of the effective resonance integral, as calculated according to CISE correlation, and the sharp decrement in the thermal fission factor. Therefore, whereas CISE correlation can be safely used for core lattice design, a way of improving the physical meaning of such recipe should be investigated.

REFERENCES

- [1] P. BACHER, R. NAUDET — “Mesures de laplaciens par la méthode du remplacement progressif”, J. Nucl. Energy, Part. A, 13, 112 (1961).
- [2] A. AMOUYAL et al. — “Rififi: méthode de calcul analytique de la condition critique et du flux d'une pile à régions variées en théorie à deux groupes et à une dimension”, Rapport CEA-1398 (1960).
- [3] R. BONALUMI, G.B. ZORZOLI — “Cocco Bill - A Criticality Calculation code”, CISE Report No. 89 (1961).
- [4] D. BRETON — “Testing Materials by the Pile Oscillation Method in the Chatillon Reactor”, P.I.C.G., 4, 127 (1956).
- [5] R. BONALUMI, S. BRUSCHETTI, G.B. ZORZOLI: “Criticality Calculations in the case of a Concentric Annuli Fuel Element Lattice — Proposed for CAN-1 Reactor in view of their Correlation with Experimental Results”, CISE Report No. 73 (1960).

Table I

AQUILON II REACTOR FEATURES

<i>Cylindrical tank</i>	
Inner diameter	2.90 m
Height	4.34 m
Wall thickness	6 mm
Bottom thickness	10 mm
Side thermal shield thickness	1 mm
<i>Graphite reflectors</i>	
Bottom reflector height	70 cm
Side reflector inner diameter	3 m
Diameter of the circle inscribed in the eight-sided outer profile	4.10 m
<i>Safety and control system</i>	
2 independent Cd safety rods (inside the core):	
diameter	60 mm
height	1 m
withdrawal speed	4.5 cm/s
introduction	by gravity
2 vertical control plates (between tank and graphite)	
maximum speed	5 cm/s
2 horizontal control plates (10 cm below the tank)	
maximum speed	5 cm/s
<i>Maximum heavy water content</i>	16.5 t
<i>Maximum uranium content</i>	15 t

Table II

7 (OF'') 7 ELEMENT CHARACTERISTICS

Fuel material	Natural uranium oxide
Fuel pellet diameter, mm	22 ± 0.05
Fuel cladding	Aluminum A 5
Fuel density, g/cm ³	10.19
Cladding density, g/cm ³	2.70

Table III
EFFECT OF COUNTERS ON REACTIVITY

Lattice pitch (cm)	Counter reactivity (pcm)	$\frac{d\rho}{dH}$ (pcm/mm)	ΔH (mm)
19	160	8.81	18.1
21	220	11.2	19.7
24	220	12.2	18.0

Table IV
REFERENCE LATTICE EXPERIMENTAL DATA

Lattice pitch (cm)	19	21	24
Extrapolated critical height H_c (cm)	177.59 \pm 0.7 1.0	166.94 \pm 0.8 0.1	171.40 \pm 1.3 1.7
α (m^{-1})	1.769 \pm 0.007 0.010	1.882 \pm 0.009 0.012	1.833 \pm 0.014 0.018
Extrapolated critical radius R_c (cm)	153.89 \pm 1.5 2.0	163.06 \pm 2.2 2.8	170.57 \pm 0.9 1.2
β (m^{-1})	1.563 \pm 0.016 0.021	1.475 \pm 0.020 0.026	1.410 \pm 0.008 0.01
$B^2 = \alpha^2 + \beta^2$ (m^{-2})	5.57 \pm 0.07 0.10	5.72 \pm 0.09 0.12	5.35 \pm 0.07 0.09
B^2 normalized to 99.8% D_2O fraction (m^{-2})	5.68 \pm 0.07 0.10	5.83 \pm 0.09 0.12	5.50 \pm 0.07 0.09
B^2 normalized to 20 °C D_2O temperature (m^{-2})	5.67 \pm 0.07 0.10	5.83 \pm 0.09 0.12	5.49 \pm 0.07 0.09

N.B. — The upper uncertainty value corresponds to a 95% confidence limit, the lower one to a 99% confidence limit.

Table V

RESULTS OF SUBSTITUTION MEASUREMENTS

Substitution Config.	4 AC el.			12 AC el.			16 AC el.			24 AC el.		
	H_c (mm)	σ_H (mm)	δH_o (mm)	H_c (mm)	σ_H (mm)	δH_o (mm)	H_c (mm)	σ_H (mm)	δH_o (mm)	H_c (mm)	σ_H (mm)	δH_o (mm)
AC-1-S-3-21	1448.9	0.2	6.6	1462.8	0.1	20.5	1468.1	0.2	25.8	1481.2	0.4	38.9
AC-2-T-1-19	1515.7	0.1	0	1515.6	0.1	— 0.1	1514.5	0.1	— 1.2	1513.1	0.1	— 2.6
AC-2-T-1-21	1441.4	0	0.4	1443.6	0.1	2.6	1445.7	0	4.7	1447.9	0.1	6.9
AC-2-T-1-24	1485.4	0.1	2.1	1491.4	0	8.1	1491.5	0.1	8.2	1498.3	0.1	15.0
AC-1-T-3-19	1542.9	0.1	19.1	1578.0	0	54.2	1591.5	0.1	67.7	1627.0	0.1	103.2
AC-1-T-3-21	1466.4	0.1	21.8	1506.6	0	62.0	1526.6	0	82.0	1564.1	0	119.5
AC-1-T-3-24	1515.5	0	28.7	1569.2	0.2	82.4	1596.4	0	109.6	1645.5	0.1	158.7
AC-1-T-0-21	1440.0	0	— 6.2	1428.6	0	—17.6	1422.7	0.2	—23.5	1414.3	0	—31.9
AC-1-T-1-21	1458.3	0	10.4	1478.3	0	30.4	1485.7	0.7	37.8	1500.7	0.1	52.8

Table VI

NUMERICAL DATA OF REFERENCE LATTICES

Lattice pitch (cm)	19	21	24
f	0.9740	0.9714	0.9668
$\bar{N}_{scM} (10^{-2} \text{ cm}^{-1})$	0.7393	0.5806	0.4220
ϕ_m/ϕ_u	1.664	1.723	1.805
\bar{D}_M (cm)	0.8235	0.8252	0.8269
L^2_M (cm ²)	111.39	142.13	195.95
\bar{D}_e (cm)	1.2011	1.2010	1.2008
$\bar{N}^*_{sUe} (10^{-2} \text{ cm}^{-1})$	0.9258	0.9436	0.9622
ϵ	1.0152	1.0152	1.0152
L_e^2 (cm ²)	129.73	127.29	124.80
$\eta_M p$	1.1556	1.1816	1.2067
$p = \frac{p \eta_M}{1.32}$	0.8755	0.8952	0.9142
K_∞	1.1426	1.1652	1.1844

Table VII
COMPUTED DATA FOR ΔB^2 CALCULATION

Configuration	ρ	S (units 10^{-3})	ΔB^2 (last value) (m^{-2})	U mean deviation σ_U	ΔB^2 deviation $\sigma_{\Delta B^2}$ (m^{-2})
AC-1-T-0-21	0.9995	-0.9627	0.213	1.3×10^{-2}	0.003
AC-1-T-1-21	0.9999	-1.0245	-0.599	2.7×10^{-2}	0.016
AC-1-T-3-19	0.9996	-0.5997	-0.932	1.9×10^{-2}	0.018
AC-1-T-3-21	1.0006	-0.0021	-1.270	3.2×10^{-3}	0.004
AC-1-T-3-24	1.0002	-0.4307	-1.340	4.4×10^{-3}	0.006
AC-1-S-3-21	1.0000	1.2010	-0.466	7.7×10^{-3}	0.004
AC-2-T-1-21	0.9997	1.5993	-0.129	1.5×10^{-2}	0.006
AC-2-T-1-24	1.0007	1.0750	-0.163	8.3×10^{-2}	0.014

Table VIII
FINAL RESULTS

Configuration	Reference buckling B^2_{ref} (m^{-2})	ΔB^2 (m^{-2})	Buckling B^2 (m^{-2})
AC-1-T-0-21	5.83 ± 0.12	0.21 ± 0.01	6.04 ± 0.12
AC-1-T-1-21	5.83 ± 0.12	-0.60 ± 0.02	5.23 ± 0.12
AC-1-T-3-19	5.67 ± 0.10	-0.93 ± 0.02	4.74 ± 0.10
AC-1-T-3-21	5.83 ± 0.12	-1.27 ± 0.02	4.56 ± 0.12
AC-1-T-3-24	5.49 ± 0.09	-1.34 ± 0.03	4.15 ± 0.09
AC-1-S-3-21	5.83 ± 0.12	-0.47 ± 0.01	5.36 ± 0.12
AC-2-T-1-19	5.67 ± 0.10	—	5.67 ± 0.10
AC-2-T-1-21	5.83 ± 0.12	-0.13 ± 0.01	5.70 ± 0.12
AC-2-T-1-24	5.49 ± 0.09	-0.16 ± 0.01	5.33 ± 0.09

Table IX

INPUT DATA FOR BUCKLING THEORETICAL EVALUATION

a) AC-I-T-0-21 (f = 0.955)

Material	Fuel		Cladding	Moderator	
Density (g/cm ³)	18.7		2.7	1.105	
Components	U ²³⁸	U ²³⁵	Al	D ₂ O	H ₂ O
Atomic or molecular %	99.28	0.72	100	99.8	0.2
$\hat{\sigma}_{aM}(b)$	2.72	661.09	0.23	1.1×10^{-3}	0.664
$\hat{\sigma}_{sM}(b)$	9.78	11.80	1.56	17.10	109.84
$\hat{\sigma}_{ac}(b)$	2.71(*)	—	0.21	1.1×10^{-3}	0.664
$\hat{\sigma}_{sc}(b)$	231.65	231.65	27.03	202.69	847.64
ξ	0.0084	0.0084	0.0723	0.507	0.948
$(1-\bar{\mu})_M$	0.9972	0.9972	0.9754	0.884	0.778
$(1-\bar{\mu})_c$	0.9972	0.9972	0.9754	0.772	0.387

(*) $\frac{1}{v}$ contribution only.

Table IX (contd.)

b) AC-1-T-1-21 and AC-1-S-3-21 ($f = 0.93$)

Material	Fuel		Cladding	Moderator		Polystyrene	
Density (g/cm ³)	18.7		2.7	1.105		{ 0.271 AC-1-T-1-21 0.511 AC-1-S-3-21	
Components	U ²³⁸	U ²³⁵	Al	D ₂ O	H ₂ O	C	H
Atomic or molecular %	99.28	0.72	100	99.8	0.2	48.54	51.46
$\hat{\sigma}_{oM}(b)$	2.72	662.76	0.23	1.1×10^{-3}	0.664	3.4×10^{-3}	0.332
$\hat{\sigma}_{sM}(b)$	9.62	11.61	1.53	16.84	109.10	5.66	52.17
$\hat{\sigma}_{oo}(b)$	2.71 (*)	—	0.21	1.1×10^{-3}	0.664	3.4×10^{-3}	0.332
$\hat{\sigma}_{so}(b)$	228.48	228.48	26.66	199.92	836.06	90.73	381.85
ξ	0.0084	0.0084	0.0723	0.507	0.948	0.158	1.00
$(1-\bar{\mu})_M$	0.9972	0.9972	0.9754	0.884	0.782	0.9444	0.773
$(1-\bar{\mu})_o$	0.9972	0.9972	0.9754	0.772	0.3874	0.9444	0.3386

(*) $\frac{1}{v}$ contribution only.

c) AC-1-T-3-19 ($f = 0.915$)

Material	Fuel		Cladding	Moderator		Polystyrene	
Density (g/cm ³)	18.7		2.7	1.105		0.511	
Components	U ²³⁸	U ²³⁵	Al	D ₂ O	H ₂ O	C	H
Atomic or molecular %	99.28	0.72	100	99.8	0.2	48.54	51.46
$\hat{\sigma}_{oM}(b)$	2.72	663.30	0.23	1.1×10^{-3}	0.664	3.4×10^{-3}	0.332
$\hat{\sigma}_{sM}(b)$	9.58	11.55	1.53	16.75	108.86	5.55	52.06
$\hat{\sigma}_{oo}(b)$	2.71 (*)	—	0.21	1.1×10^{-3}	0.664	3.4×10^{-3}	0.332
$\hat{\sigma}_{so}(b)$	227.47	227.47	26.54	199.03	832.34	89.09	380.15
ξ	0.0084	0.0084	0.0723	0.507	0.948	0.158	1.00
$(1-\bar{\mu})_M$	0.9972	0.9972	0.9754	0.884	0.783	0.9444	0.774
$(1-\bar{\mu})_o$	0.9972	0.9972	0.9754	0.772	0.3874	0.9444	0.3386

(*) $\frac{1}{v}$ contribution only.

Table IX (contd.)

d) AC-1-T-3-21 ($f = 0.910$)

Material	Fuel		Cladding	Moderator		Polystyrene	
Density (g/cm ³)	18.7		2.7	1.105		0.511	
Components	U ²³⁸	U ²³⁵	Al	D ₂ O	H ₂ O	C	H
Atomic or molecular %	99.28	0.72	100	99.8	0.2	48.54	51.46
$\hat{\sigma}_{aM}(b)$	2.72	663.45	0.23	1.1×10^{-3}	0.664	3.4×10^{-3}	0.332
$\hat{\sigma}_{sM}(b)$	9.56	11.54	1.52	16.73	108.80	5.54	52.04
$\hat{\sigma}_{ac}(b)$	2.71 (*)	—	0.21	1.1×10^{-3}	0.664	3.4×10^{-3}	0.332
$\hat{\sigma}_{sc}(b)$	227.20	227.20	26.51	198.80	831.37	88.99	379.71
ξ	0.0084	0.0084	0.0723	0.507	0.948	0.158	1.00
$(1-\bar{\mu})_M$	0.9972	0.9972	0.9754	0.884	0.784	0.9444	0.775
$(1-\bar{\mu})_c$	0.9972	0.9972	0.9754	0.772	0.3874	0.9444	0.3386

(*) $\frac{1}{v}$ contribution only.

e) AC-1-T-3-24 ($f = 0.905$)

Material	Fuel		Cladding	Moderator		Polystyrene	
Density (g/cm ³)	18.7		2.7	1.105		0.511	
Components	U ²³⁸	U ²³⁵	Al	D ₂ O	H ₂ O	C	H
Atomic or molecular %	99.28	0.72	100	99.8	0.2	48.54	51.46
$\hat{\sigma}_{aM}(b)$	2.72	663.57	0.23	1.1×10^{-3}	0.664	3.4×10^{-3}	0.332
$\hat{\sigma}_{sM}(b)$	9.55	11.52	1.52	16.71	108.74	5.53	52.01
$\hat{\sigma}_{ac}(b)$	2.71 (*)	—	0.21	1.1×10^{-3}	0.664	3.4×10^{-3}	0.332
$\hat{\sigma}_{sc}(b)$	226.96	226.96	26.48	198.59	830.50	88.89	379.31
ξ	0.0084	0.0084	0.0723	0.507	0.948	0.158	1.00
$(1-\bar{\mu})_M$	0.9972	0.9972	0.9754	0.884	0.784	0.9444	0.775
$(1-\bar{\mu})_c$	0.9972	0.9972	0.9754	0.772	0.3874	0.9444	0.3386

(*) $\frac{1}{v}$ contribution only.

Table IX (contd.)

f) AC-2-T-1-19 and AC-2-T-1-21 ($f = 0.940$)

Material	Fuel		Cladding	Moderator		Polistyrene	
Density (g/cm ³)	18.7		2.7	1.105		0.271	
Components	U ²³⁸	U ²³⁵	Al	D ₂ O	H ₂ O	C	H
Atomic or molecular %	99.28	0.72	100	99.8	0.2	48.54	51.46
$\hat{\sigma}_{aM}(b)$	2.72	662.24	0.23	1.1×10^{-3}	0.664	3.4×10^{-3}	0.332
$\hat{\sigma}_{sM}(b)$	9.67	11.67	1.54	16.92	109.32	5.60	52.27
$\hat{\sigma}_{ae}(b)$	2.71 (*)	—	0.21	1.1×10^{-3}	0.664	3.4×10^{-3}	0.332
$\hat{\sigma}_{sc}(b)$	229.44	229.44	26.77	200.76	839.55	89.86	383.45
ξ	0.0084	0.0084	0.0723	0.507	0.948	0.158	1.00
$(1-\bar{\mu})_M$	0.9972	0.9972	0.9754	0.884	0.781	0.9444	0.772
$(1-\bar{\mu})_c$	0.9972	0.9972	0.9754	0.772	0.3874	0.9444	0.3386

(*) $\frac{1}{v}$ contribution only.

Table IX (end)
g) AC-2-T-1-24 ($f = 0.935$)

Material	Fuel		Cladding	Moderator		Polistyrene	
Density (g/cm ³)	18.7		2.7	1.105		0.271	
Components	U ²³⁸	U ²³⁵	Al	D ₂ O	H ₂ O	C	H
Atomic or molecular %	99.28	0.72	100	99.8	0.2	48.54	51.46
$\hat{\sigma}_{aM}(b)$	2.72	662.52	0.23	1.1×10^{-3}	0.664	3.4×10^{-3}	0.332
$\hat{\sigma}_{sM}(b)$	9.65	11.64	1.54	16.88	109.20	5.59	52.22
$\hat{\sigma}_{ae}(b)$	2.71 (*)	—	0.21	1.1×10^{-3}	0.664	3.4×10^{-3}	0.332
$\hat{\sigma}_{sc}(b)$	228.92	228.92	26.71	200.31	837.67	89.66	382.59
ξ	0.0084	0.0084	0.0723	0.507	0.948	0.158	1.00
$(1-\bar{\mu})_M$	0.9972	0.9972	0.9754	0.884	0.781	0.9444	0.772
$(1-\bar{\mu})_c$	0.9972	0.9972	0.9754	0.772	0.3874	0.9444	0.3386

(*) $\frac{1}{v}$ contribution only.

Table X
THEORETICAL CELL PARAMETERS AND BUCKLINGS
OF TESTED CONFIGURATIONS

Configuration	f	η_{calc}	ε	q	$K_{\infty} = \frac{1}{yf\eta_{calc}\varepsilon q}$	L^2_{rM} (cm ²)	L^2_{zM} (cm ²)	L^2_{re} (cm ²)	L^2_{ze} (cm ²)	B^2 (m ⁻²)
AC-1-T-0-21	0.9545	1.3181	1.0346	0.9318	1.1748	151.36	154.62	136.62	141.20	6.02
AC-1-T-1-21	0.9338	1.3194	1.0333	0.9257	1.1415	149.25	149.83	121.37	122.00	5.23
AC-1-T-3-19	0.9191	1.3199	1.0322	0.9105	1.1044	115.18	116.04	112.06	112.88	4.69
AC-1-T-3-21	0.9161	1.3201	1.0322	0.9252	1.1187	147.70	148.59	112.34	113.00	4.59
AC-1-T-3-24	0.9110	1.3202	1.0322	0.9415	1.1321	204.69	205.61	112.61	113.12	4.13
AC-1-S-3-21	0.9364	1.3194	1.0322	0.9259	1.1438	150.97	152.95	113.58	115.33	5.43
AC-2-T-1-19	0.9443	1.3190	1.0414	0.8956	1.1252	111.30	111.84	123.36	124.21	5.48
AC-2-T-1-21	0.9416	1.3190	1.0414	0.9139	1.1450	141.67	142.22	121.43	122.12	5.55
AC-2-T-1-24	0.9369	1.3192	1.0414	0.9335	1.1639	194.69	195.25	119.47	119.98	5.16

Table XI
COMPARISON BETWEEN CALCULATED AND EXPERIMENTAL BUCKLINGS

Configuration	B^2 (m ⁻²)			B^2 (m ⁻²) Preliminary evaluation
	Experimental	Calculated		
		a	b	
AC-1-T-0-21	6.04 ± 0.12	6.02	6.01	5.93
AC-1-T-1-21	5.23 ± 0.12	5.23	4.85	5.05
AC-1-T-3-19	4.74 ± 0.10	4.69	3.70	4.40
AC-1-T-3-21	4.56 ± 0.12	4.59	4.09	4.26
AC-1-T-3-24	4.15 ± 0.09	4.13	4.05	3.79
AC-1-S-3-21	5.36 ± 0.12	5.43	4.95	5.10
AC-2-T-1-19	5.67 ± 0.10	5.48	4.47	5.23
AC-2-T-1-21	5.70 ± 0.12	5.55	5.05	5.35
AC-2-T-1-24	5.33 ± 0.09	5.16	5.10	4.97

Calculation a) performed after CISE correlation

Calculation b) performed with $\gamma=1$ and Hellstrand's effective resonance integral.

Table XII**THEORETICAL BUCKLINGS OF THE CONFIGURATIONS
USED FOR STUDYING THE HYDROGEN EFFECT**

Configuration	Buckling (m^{-2})
AC-1-T-0-19	5.83
AC-1-T-0-21	6.02
AC-1-T-0-24	5.42
AC-1-T-1-19	5.28
AC-1-T-1-21	5.23
AC-1-T-1-24	4.79
AC-1-T-3-19	4.69
AC-1-T-3-21	4.59
AC-1-T-3-24	4.13
AC-2-T-0-19	6.05
AC-2-T-0-21	6.14
AC-2-T-0-24	5.79
AC-2-T-1-19	5.48
AC-2-T-1-21	5.55
AC-2-T-1-24	5.16
AC-2-T-3-19	4.92
AC-2-T-3-21	4.90
AC-2-T-3-24	4.57



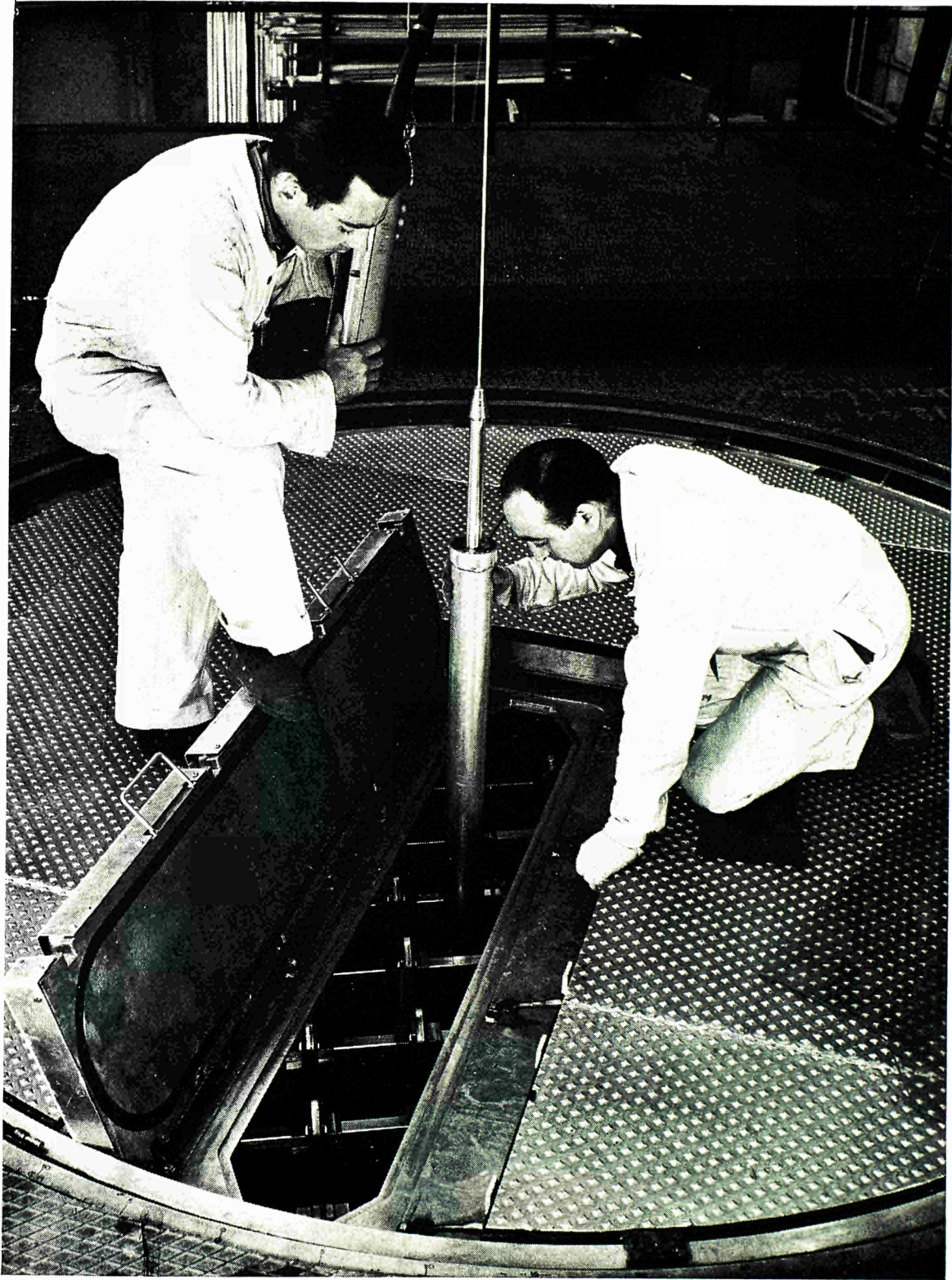


Fig. 1 - Charging of fuel elements in Aquilon II.

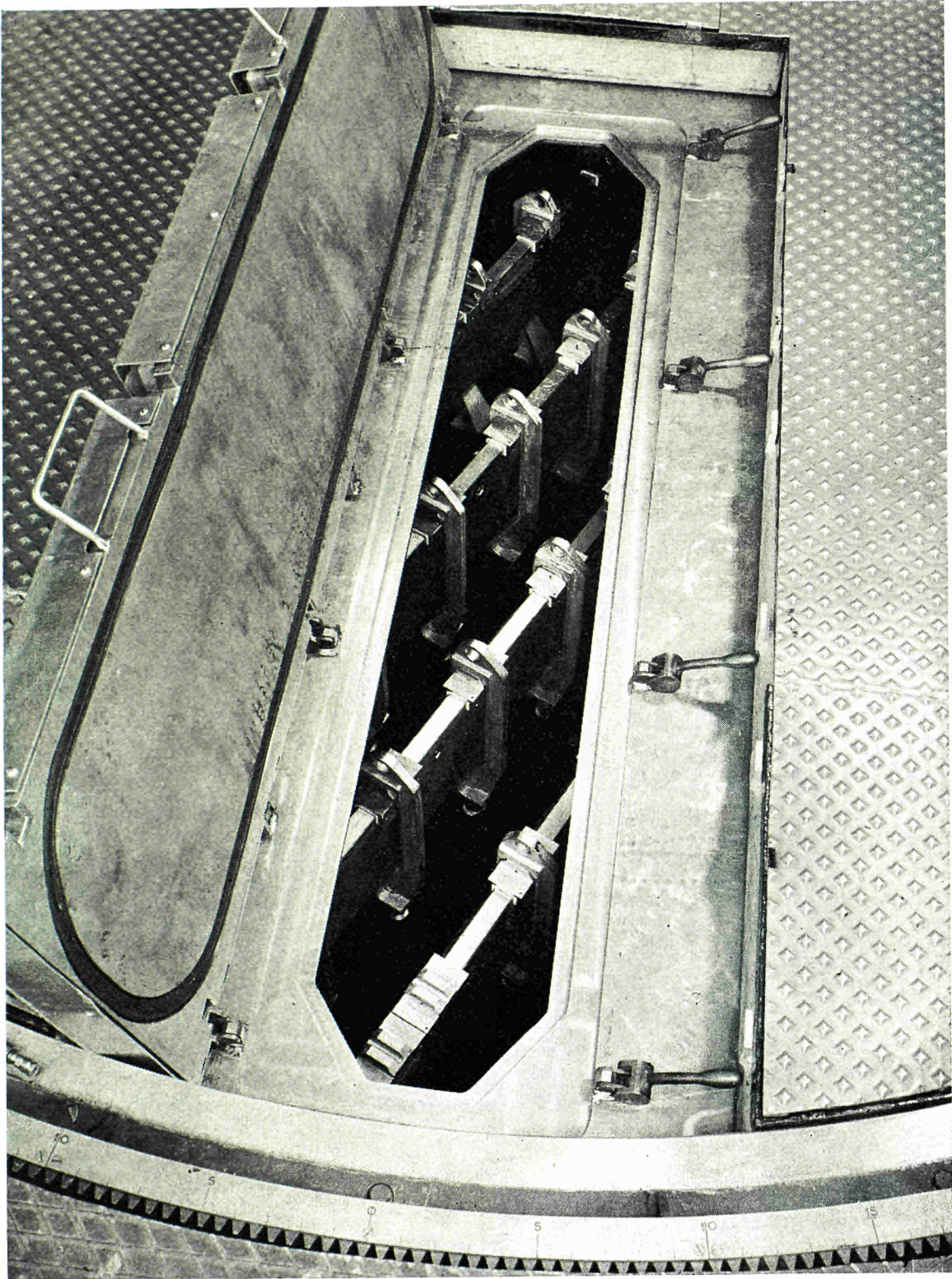


Fig. 2 - Fuel element hanging.

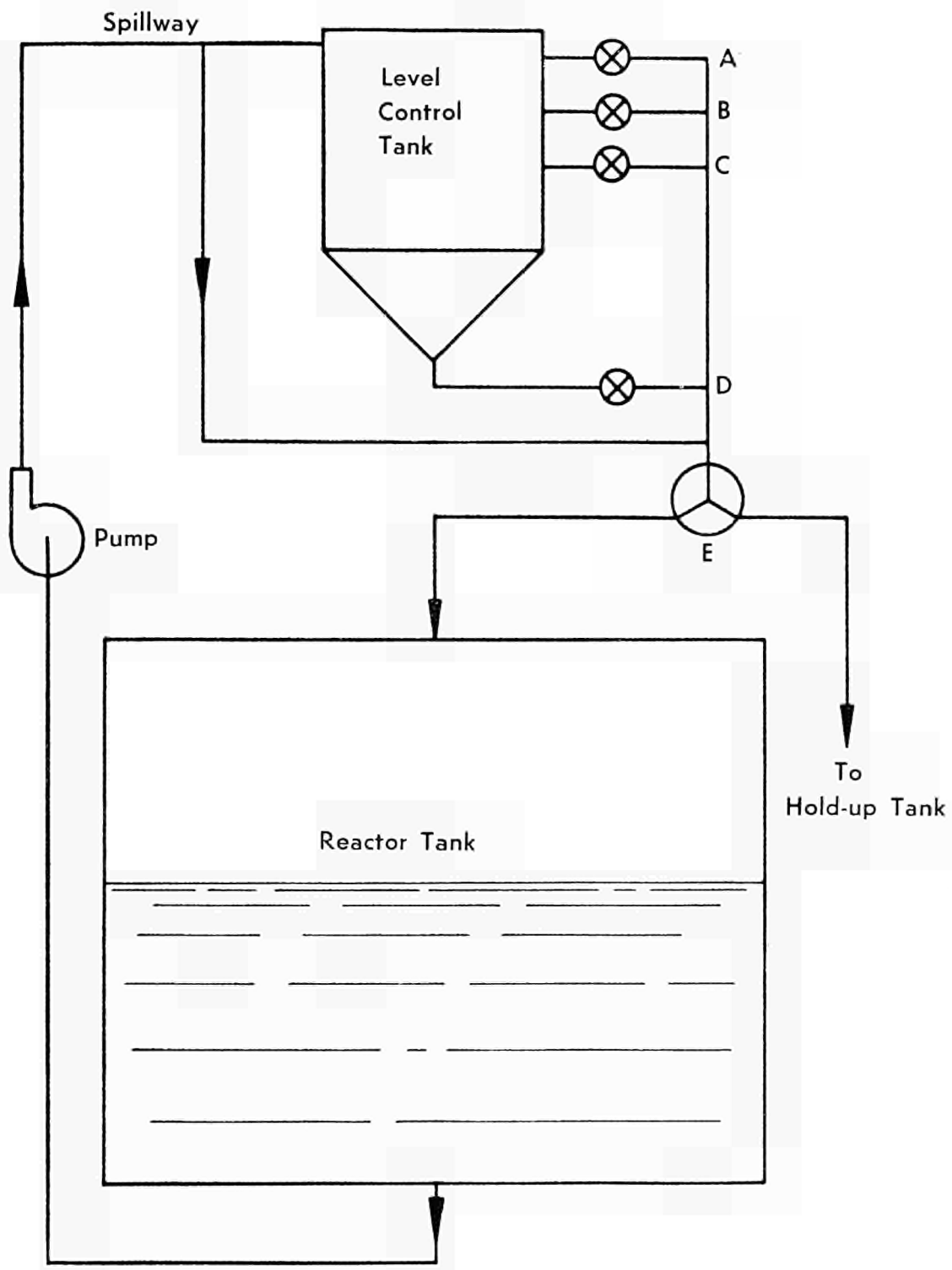


Fig. 3 — Heavy water level variation system.

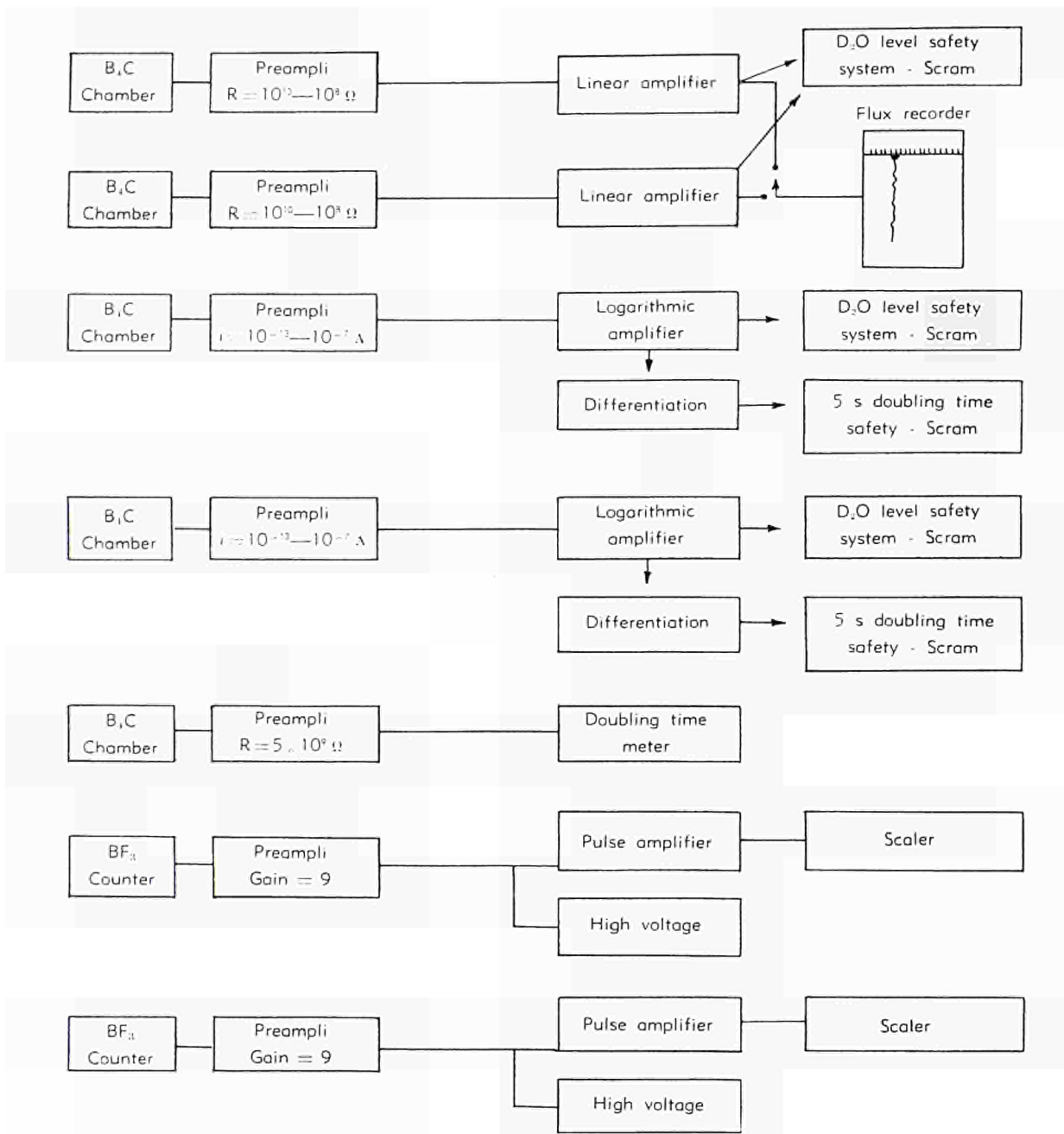


Fig. 1.

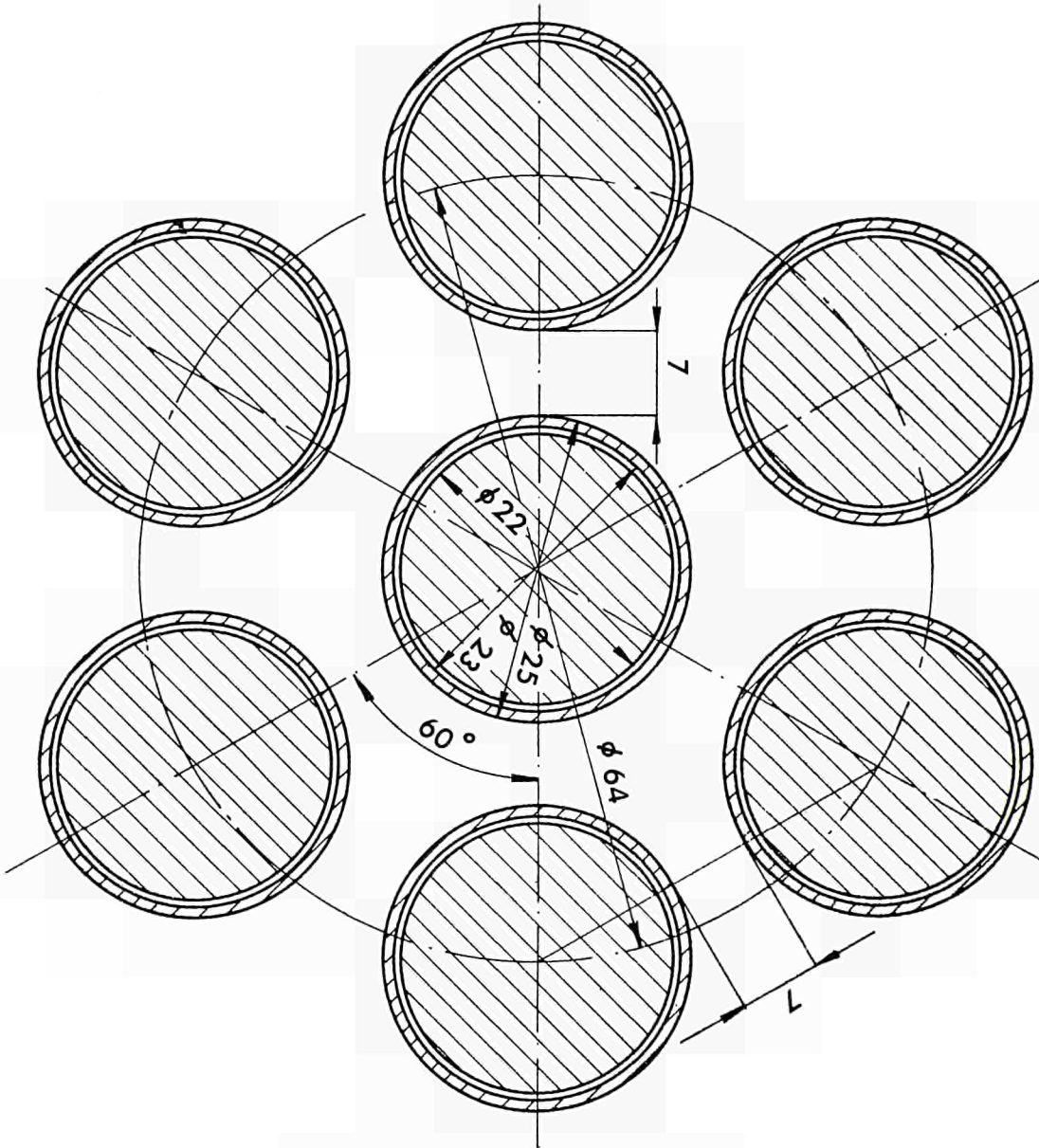


Fig. 5 — Reference lattice fuel element.

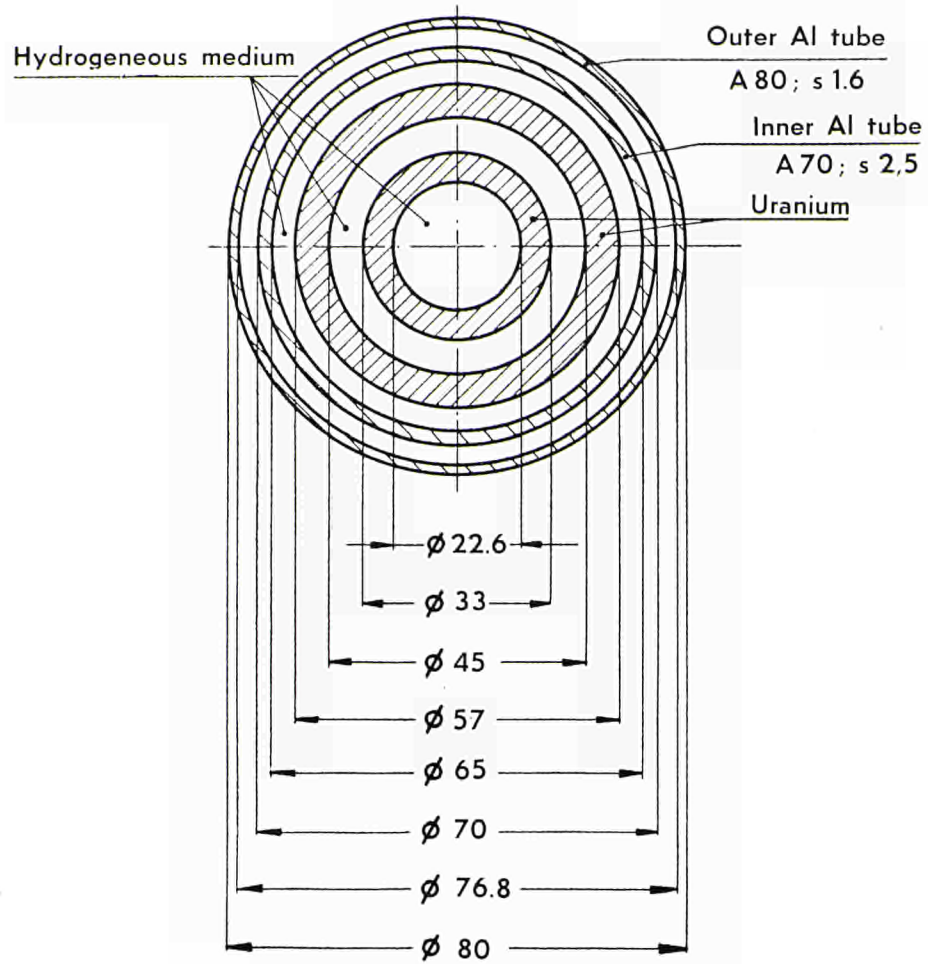


Fig. 6 — AC-1 element cross section.

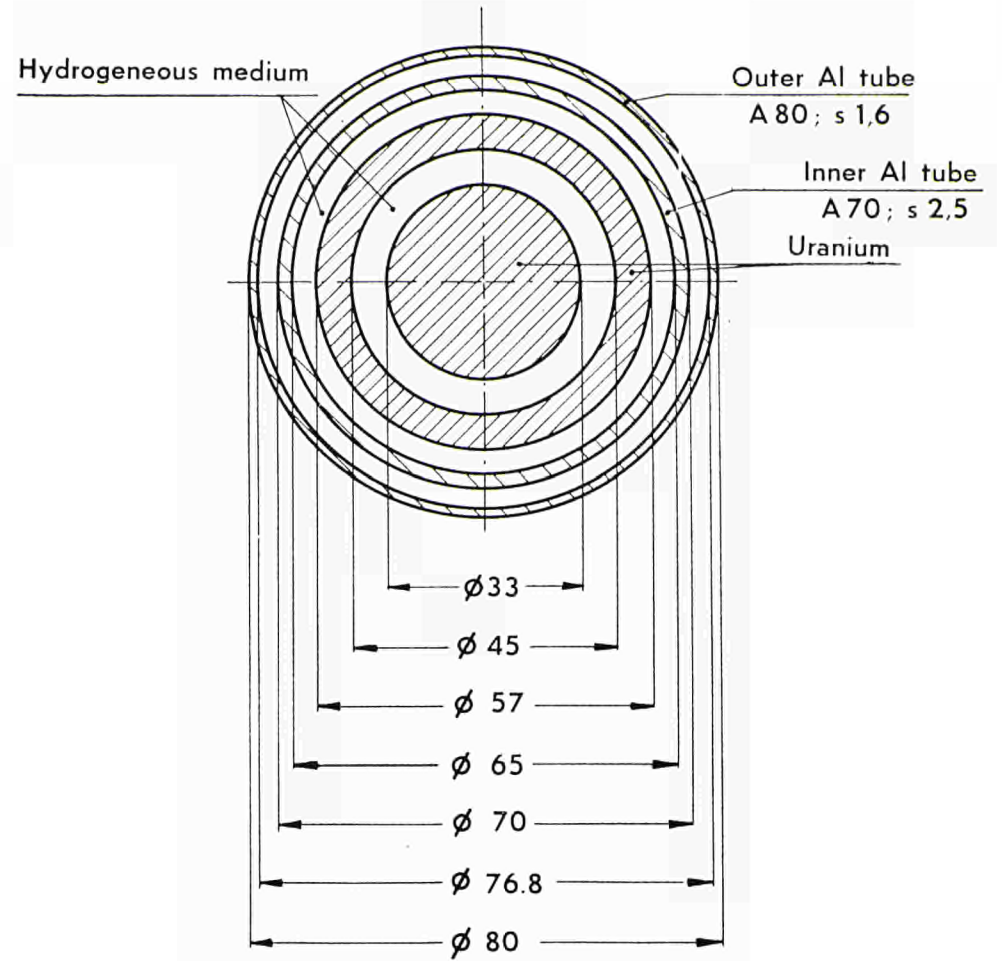


Fig. 7 — AC-2 element cross section.



Fig. 8 - AC-1 top view.

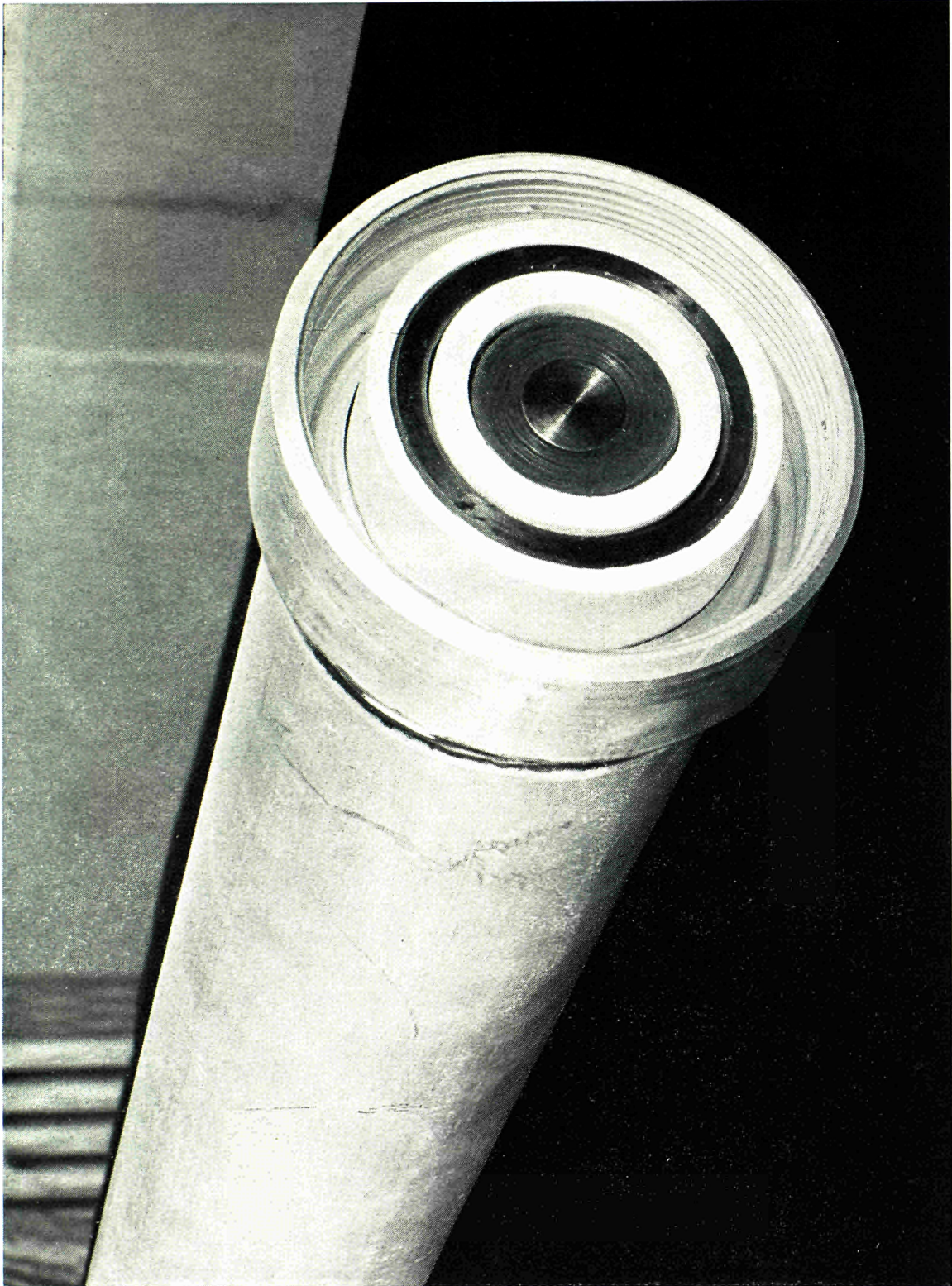


Fig. 9 - AC-2 top view.

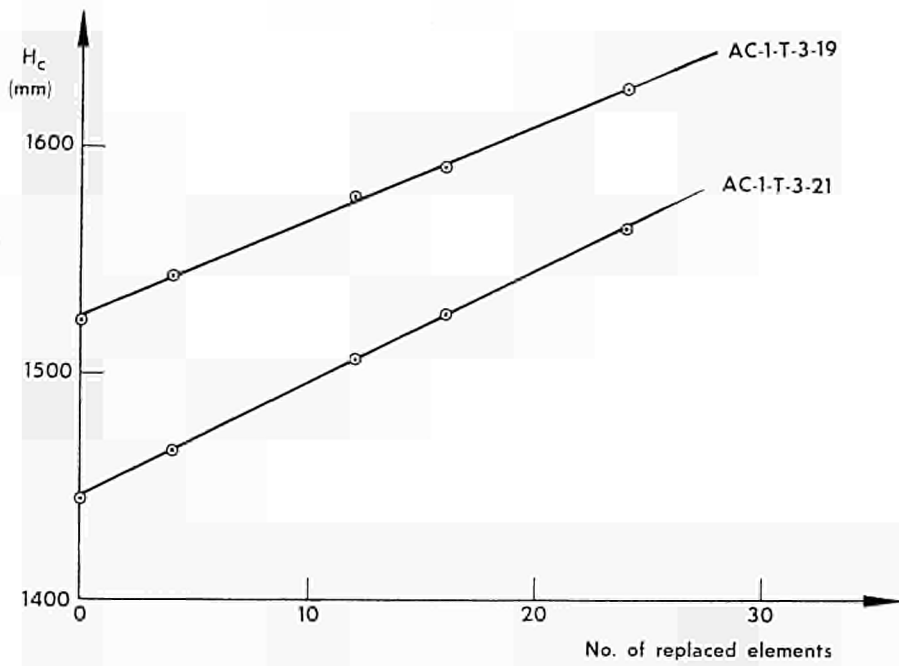


Fig. 10 — Critical height vs. number of replaced elements.

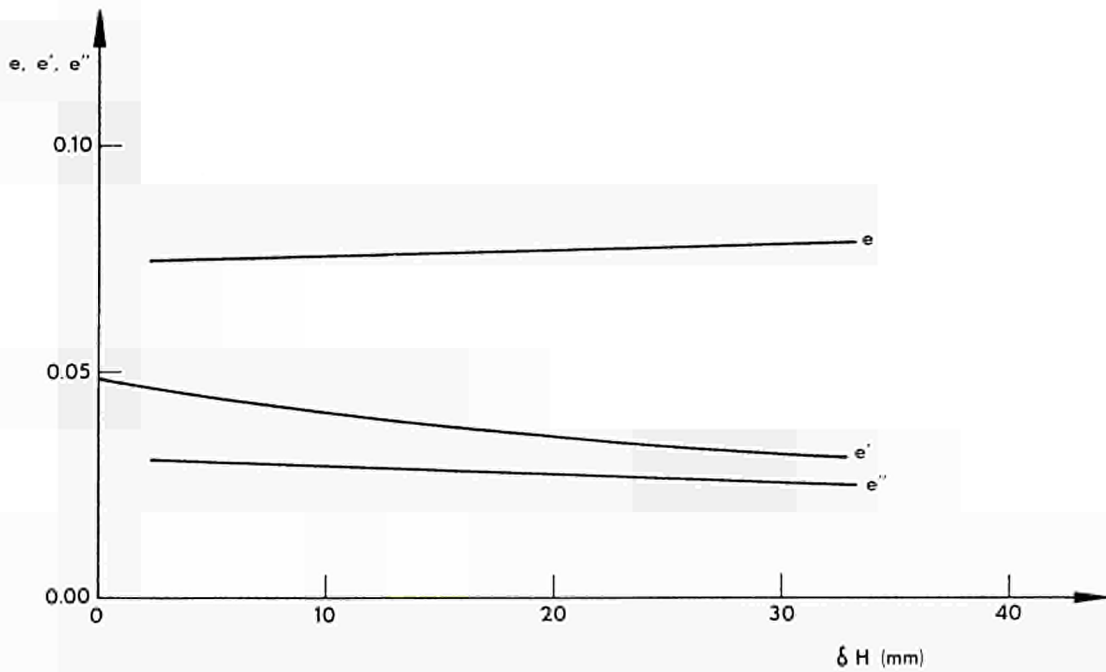


Fig. 11 — Reflector coefficients vs. δH , 19 cm lattice pitch.

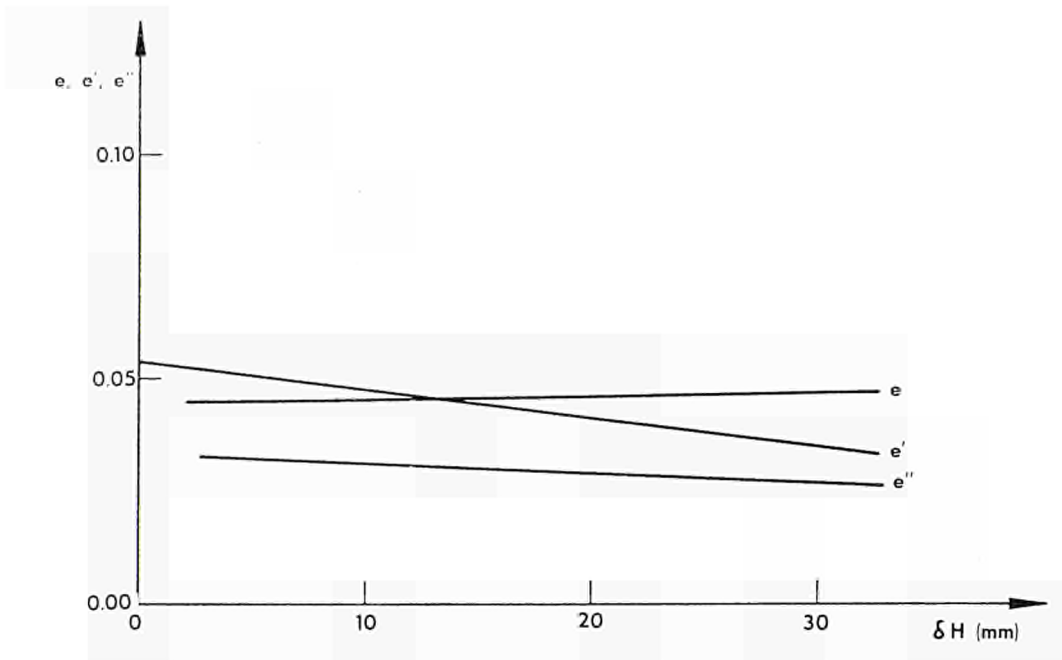


Fig. 12 — Reflector coefficients vs. δH , 21 cm lattice pitch.

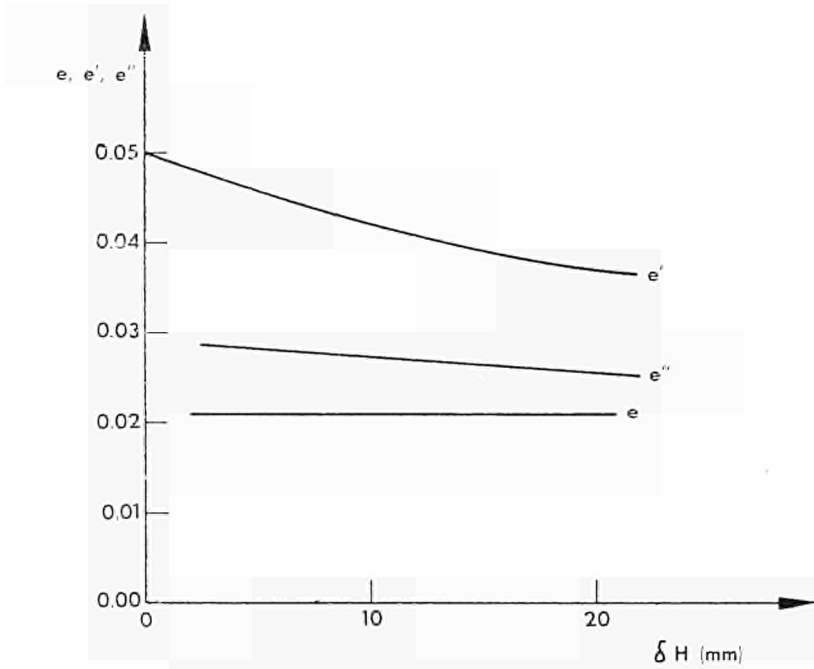


Fig. 13 — Reflector coefficients vs. δH , 24 cm lattice pitch.

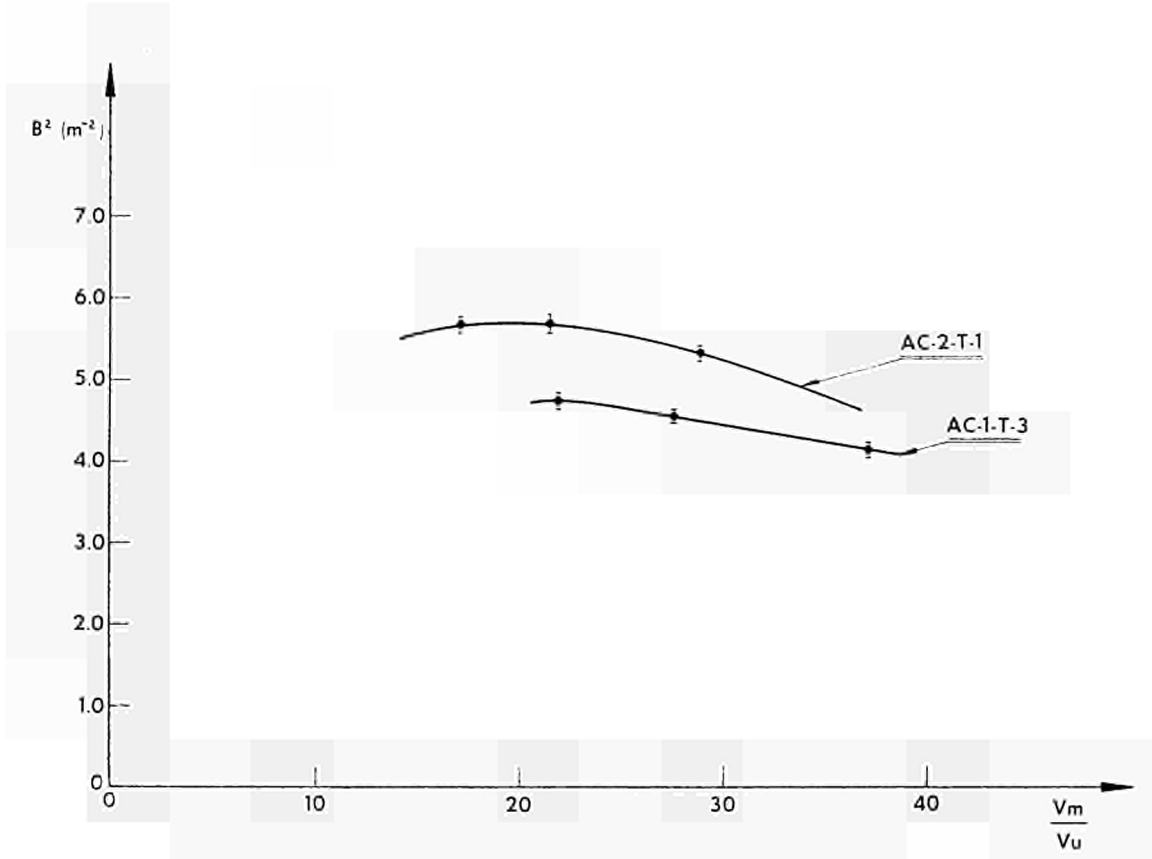


Fig. 14 — AC-2-T-1 and AC-1-T-3 experimental bucklings vs. V_m/V_u .



CDNA00025ENC